

**ÇUKUROVA UNIVERSITY  
INSTITUTE OF NATURAL AND APPLIED SCIENCES**

**MSc THESIS**

**Osman Cenk CANDEMİR**

**INVESTIGATION OF PROPANOL-ADBLUE BLENDS AS A  
REDUCTANT AGENT IN A SCR SYSTEM**

**DEPARTMENT OF AUTOMOTIVE ENGINEERING**

**ADANA, 2019**

**ÇUKUROVA UNIVERSITY  
INSTITUTE OF NATURAL AND APPLIED SCIENCES**

**INVESTIGATION OF PROPANOL-ADBLUE BLENDS AS A  
REDUCTANT AGENT IN A SCR SYSTEM**

**Osman Cenk CANDEMİR**

**MSc THESIS**

**DEPARTMENT OF AUTOMOTIVE ENGINEERING**

We certify that the thesis titled above was reviewed and approved for the award of degree of the Master of Science by the board of jury on 21/11/2019.

.....  
Prof. Dr.Ali KESKİN  
SUPERVISOR

.....  
Prof. Dr.Abdülkadir YAŞAR  
MEMBER

.....  
Assoc. Prof. Dr.Erinç ULUDAMAR  
MEMBER

This MSc Thesis is written at the Department of Institute of Natural and Applied Sciences of Çukurova University.

**Registration Number:**

**Prof. Dr. Mustafa GÖK  
Director  
Institute of Natural and Applied Sciences**

**Note:** The usage of the presented specific declarations, tables, figures, and photographs either in this thesis or in any other reference without citation is subject to "The law of Arts and Intellectual Products" number of 5846 of Turkish Republic.

## ABSTRACT

### MSc THESIS

# INVESTIGATION OF PROPANOL-ADBLUE BLENDS AS A REDUCTANT AGENT IN A SCR SYSTEM

**Osman Cenk CANDEMİR**

**ÇUKUROVA UNIVERSITY  
INSTITUTE OF NATURAL AND APPLIED SCIENCES  
DEPARTMENT OF AUTOMOTIVE ENGINEERING**

Supervisor : Prof. Dr. Ali KESKİN  
Year: 2019, Pages: 83  
Jury : Prof. Dr. Ali KESKİN  
: Prof. Dr. Abdülkadir YAŞAR  
: Assoc. Prof. Dr. Erineç ULUDAMAR

In this study, Ag-Pd-Ti based catalyst was synthesized with the impregnation method for hydrocarbon-selective catalytic reduction (HC-SCR) system. In this system, a mixture of propanol and adblue was used as reducing agents and the effect of the synthesized catalyst on NO<sub>x</sub> conversion efficiency was investigated. The analysis done by SEM, XRD, and BET revealed the structural and chemical properties of the catalysts. In the SCR exhaust test performance system, experiments in a temperature ranging from 170°C to 300°C, and 1 space velocity SV (30000h<sup>-1</sup>) were conducted using the prepared catalyst. The tests were conducted using 2 cylinders, V-type diesel motor with constant speed(3000r/m), and in 4 different engine loads (1, 2, 3 and 4 KW). In conclusion, NO<sub>x</sub> conversion rates changed approximately between 42% and 68%. The highest NO<sub>x</sub> conversion rate recorded in the tests was 68,1% at 4KW engine load, 100% propanol spraying and SV=30000h<sup>-1</sup>.

**Keywords:** NO<sub>x</sub>, SCR, exhaust emission, Reductants, Diesel motor

**ÖZ**

**YÜKSEK LİSANS TEZİ**

**SCR SİSTEMİNDE İNDİRGEYİCİ OLARAK PROPANOL VE  
ADBLUE KARIŞIMININ ARAŞTIRILMASI**

**Osman Cenk CANDEMİR**

**ÇUKUROVA ÜNİVERSİTESİ  
FEN BİLİMLERİ ENSTİTÜSÜ  
OTOMOTİV MÜHENDİSLİĞİ ANABİLİM DALI**

Danışman : Prof.Dr. Ali KESKİN

Yıl: 2019, Sayfa: 83

Jüri : Prof.Dr. Ali KESKİN

: Prof.Dr. Abdülkadir YAŞAR

: Doç.Dr. Erineç ULUDAMAR

Bu çalışmada, HC-SCR sistemi için Ag-Pd-Ti esaslı katalizör emdirme yöntemiyle sentezlenmiştir. Bu sistemde indirgeyici olarak propanol ve adblue karışımı kullanılmış ve üretilen katalizörün NO<sub>x</sub> dönüşüm verimliliği üzerindeki etkisi incelenmiştir. Katalizöre ait SEM, XRD ve BET analizleri gerçekleştirilerek yapısal ve kimyasal özellikleri belirlenmiştir. SCR egzoz performans test sisteminde üretilen katalizör kullanılarak 170°C -300°C sıcaklık aralığında ve 1 SV'de (30000h<sup>-1</sup>) deneyler yapılmıştır. Testler 2 silindirli V-tipi bir dizel motor kullanılarak sabit motor devrinde (3000 d/dk) ve 4 farklı motor yüklemesinde (1, 2, 3 ve 4 KW) gerçekleştirilmiştir. Bu testlerle, SCR katalizörünün NO<sub>x</sub> emisyonu üzerindeki etkisi tespit edilmiştir. NO<sub>x</sub> dönüşüm oranlarının 42% ile 68% arasında olduğu tespit edilmiştir. En yüksek NO<sub>x</sub> dönüşüm oranı 4 KW yük durumunda, %100 propanol püskürtülerek ve SV=30000h<sup>-1</sup> değerinde yaklaşık 68,1% olarak elde edilmiştir.

**Anahtar Kelimeleri:** NO<sub>x</sub>, SCR, İndirgeyici, Dizel

## GENİŞLETİLMİŞ ÖZET

Çevreye ve İnsan sağlığına ciddi zararlar vermekte olan NO<sub>x</sub> emisyonları, iklimsel değişikliği ve küresel ısınmanın en temel kaynakları arasında gösterilmektedir. Genel olarak tüm yaşanan çevrede, NO<sub>x</sub> emisyonlarının etkisinin azaltılması ve yok edilmesine yönelik çok sayıda talimatlar ve kurallar geliştirilmektedir. Çevreye salınan NO<sub>x</sub> emisyonları en çok dizel motorlu taşıtlarının egzoz dumanında bulunmaktadır. Bu emisyonlar sadece dizel motorları için değil yaşayan tüm canlılar için, yani dünya için ciddi bir problem olmuştur. Hükümetlerin uyguladığı emisyon standartlarının her geçen gün sıkılaşmasıyla birlikte NO<sub>x</sub> emisyonlarının çevre ve insan sağlığı üzerindeki olumsuz etkileri nedeniyle otomotiv sektöründe taşıt üretimini durdurma veya dizel motor üzerindeki ar-ge çalışmalarını sonlandırma kararı verilmektedir. Fakat benzin motorlu taşıtlarla kıyaslandığında, Dizel motorlardaki yüksek dayanıklılığı, verimlilik ve düşük yakıt tüketimi gibi özellikler motoru avantajlı hale getirmektedir. Benzinli motora kıyasla, bilhassa ağır taşıma hizmet taşıtlarında dizel motorların saf dışı bırakılması oldukça zor görülmektedir. Bunun için otomotiv üreticileri ve araştırmacıları NO<sub>x</sub> emisyonlarını azaltmak ve emisyon standart değerlerini sağlamaya yönelik bir arayış içerisine sokulmuşlardır.

Çok sayıda sistem bu amaç için geliştirilmiş, uygulamalar yapılmış ancak bu sistemler emisyonun azalmasına yönelik beklenen düşüşü gerçekleştirilememiştir. NO<sub>x</sub> emisyonlarının azaltılması bir tek seçici katalitik indirgeyici (SCR) teknolojisiyle sağlanmıştır. SCR sistemi teknoloji 1970'li yıllara dayanmaktadır. Bu sistemde NO<sub>x</sub> emisyonları bir indirgeyici kullanılarak azot (N<sub>2</sub>) ve suya dönüştürülmektedir. Amonyak, SCR sisteminde en çok kullanılan indirgeyicilerden biridir. Amonyak %33 oranında üre çözeltisi ((NH<sub>2</sub>)<sub>2</sub>CO), ve %67 oranında saf suyundan (H<sub>2</sub>O) oluşan ve AdBlue olarak adlandırılan sulu üre çözeltisinin egzoz gazına püskürtülmesiyle elde edilmektedir. SCR sistemlerinde en yaygın olarak kullanılan katalizör V<sub>2</sub>O<sub>5</sub>-WO<sub>3</sub>/TiO<sub>2</sub> yapısına sahip, ve indirgeyici olarak Adblue

solüsyonudur. NO<sub>x</sub> emisyonları özellikle 350°C -450°C egzoz gazı sıcaklıklarında hayli yüksek oranlarda azaltılmaktadır. Fakat 250°C'nin altındaki düşük egzoz gazı sıcaklıklarında dönüşüm verimliliği azaldığı ve katalizör yüzeylerinde amonyak birikmesi gözlemlenmektedir.

Bu çalışmada üretimi gerçekleştirilen Ag-Pd-Ti katalizöründe NO<sub>x</sub> emisyonlarının propanol ve adblue kullanılarak seçici katalitik indirgenmesi üzerine odaklanılmıştır. Katalizöre ait analizler gerçekleştirilerek özel olarak tasarlanmış egzoz sistemi aracılığıyla farklı motor yükü, space velocity ve egzoz gazı sıcaklıklarında propanol-adblue karışımının Ag-Pd-Ti katalizörü kullanılarak NO<sub>x</sub> dönüşüm verimliliği üzerindeki etkileri deneysel olarak araştırılmıştır. Katalizör üretimi, Çukurova Üniversitesi Otomotiv Mühendisliğine ait laboratuvarların altyapısı kullanılarak gerçekleştirilmiştir. Katalizör üretiminde, hazır olarak temin edilen 400 cpsi kare gözeneğe sahip kordiyerit (2Al<sub>2</sub>O<sub>3</sub>-5SiO<sub>2</sub>-2MgO) ve monolith ana taşıyıcı yapı kullanıldı.

HC-SCR sistemi için Ag-Pd-Ti esaslı katalizör emdirmeye yöntemiyle sentezlenmiştir. İlk önce Kordiyerit tartırıldı sonra fırında 110°C sıcaklıkta 1 saat boyunca ısıtıldı. Kordiyerit yapının kaplanması amacıyla gümüş esaslı solüsyon IV hazırlandı. Solüsyon hazırlamak için 500 ml distile suyun içine 5,91g gümüş nitrat (AgNO<sub>3</sub>), 50g titanyum dioksitin (TiO<sub>2</sub>) yanı sıra 17,3g oksalik asit (C<sub>2</sub>H<sub>2</sub>O<sub>4</sub>·2H<sub>2</sub>O) eklenerek ultrasonik karıştırıcıda yaklaşık 20 dakika boyunca karıştırıldı. Elde edilen solüsyona kordiyerit malzeme daldırıldı. Daldırma işleminden sonra kordiyerit malzeme fırında 110°C sıcaklıkta 1 saat boyunca kurutuldu. Daha sonra bu malzemeler 550°C sıcaklıkta 4 saat kalsine edildi. Böylece katalist yapıların üretimi gerçekleştirildi.

Sonuç olarak, katalizöre ait SEM, XRD ve BET analizleri gerçekleştirilerek yapısal ve kimyasal özellikleri belirlenmiştir. SCR egzoz performans test sisteminde üretilen katalizör kullanılarak 170°C-300°C sıcaklık aralığında ve 1 SV'de (30000h<sup>-1</sup>) deneyler yapılmıştır. Testler 2 silindri V-tipi bir dizel motor kullanılarak sabit motor devrinde (3000 d/dk) ve 4 farklı motor

yüklemesinde (1, 2, 3 ve 4 KW) gerçekleştirilmiştir. Bu testlerle, SCR katalizörünün NO<sub>x</sub> emisyonu üzerindeki etkisi tespit edilmiştir. NO<sub>x</sub> dönüşüm oranlarının 42% ile 68% arasında olduğu tespit edilmiştir. En yüksek NO<sub>x</sub> dönüşüm oranı 4 KW yük durumunda, %100 propanol püskürtülerek ve SV=30000h<sup>-1</sup> değerinde yaklaşık 68,1% olarak elde edilmiştir.







## **ACKNOWLEDGEMENTS**

I owe my deepest gratitude to all those who gave me the opportunity to complete this thesis. First, I have to thank my supervisor Prof. Dr. Ali Keskin for his patience and support allowing me to work independently on my chosen area of research.

I gratefully thank Research Assistant Mr. Himmet Özarlan for his generosity in his time and the constant help I particularly needed through the researching and writing.

Finally, I would like to express my gratitude to my family. Without their support, this work would never have been completed.

<b>TABLE OF CONTENTS</b>	<b>PAGES</b>
ABSTRACT.....	I
ÖZ .....	II
GENİŞLETİLMİŞ ÖZET .....	III
ACKNOWLEDGEMENTS.....	VII
TABLE OF CONTENTS.....	VIII
LIST OF TABLES .....	XII
LIST OF FIGURES .....	XIV
LIST OF ABBREVIATIONS AND NOMENCLATURE.....	XVI
1. INTRODUCTION .....	1
2. DIESEL ENGINES AND EMISSIONS.....	5
2.1 Diesel Engines .....	5
2.2 Emissions from Diesel Engines .....	7
2.2.1 Sulfur Oxides (SO <sub>x</sub> ) .....	7
2.2.2 Particulate Matter (PM) .....	8
2.2.3 Carbon Dioxide (CO <sub>2</sub> ) .....	9
2.2.4 Carbon Monoxide (CO) .....	10
2.2.5 Hydrocarbons (HC).....	11
2.2.6 Oxides of Nitrogen (NO <sub>x</sub> ) .....	12
3. EMISSIONS REGULATION AND MINIMIZATION .....	15
3.1 Emissions Regulations .....	15
3.2 Emissions Control Systems.....	18
3.2.1 Exhaust Gas Recirculation (EGR) .....	18
3.2.2 Diesel Particulate Filters .....	19
3.2.3 Three-Way Catalytic Converter (TWC).....	21
3.2.4 Diesel Oxidation Catalyst .....	23
3.2.5 Selective Catalytic Reduction .....	25
3.2.5.1 Hyrdocarbons SCR (HC-SCR) .....	27

3.2.5.2 Reductants for HC-SCR.....	27
3.2.5.3 Catalysts for HC-SCR.....	30
3.3 Objective of The Study .....	31
4. LITERATURE REVIEW .....	33
5. MATERIALS AND METHODS.....	39
5.1 Catalyst Preparation.....	39
5.1.1 Cordierite Specifications.....	40
5.2. Catalyst Characterization Equipment and Technical Properties:.....	41
5.2.1. X-ray Diffraction (XRD) .....	41
5.2.2. BET Analysis.....	43
5.2.3. SEM Analysis .....	44
5.3 Chemical Properties of Materials Used in Catalyst Preparation.....	45
5.3.1. Propanol.....	45
5.3.2. AdBlue .....	46
5.3.3. Palladium .....	47
5.4 Technical Properties of The Devices Used in Catalyst Preparation.....	47
5.4.1. RADWAG AS 220. R2.....	48
5.4.2. Ultrasonic Processor .....	48
5.4.3 Sintering Oven .....	50
5.4.4. Drying Oven.....	51
5.5. NO <sub>x</sub> Emissions Measurement System.....	52
5.5.1 Performance Test System Overview.....	52
5.5.2 Technical Properties of Test System Components.....	55
5.5.2.1 NO <sub>x</sub> Sensors .....	55
5.5.2.2. Arduino MEGA 2560.....	56
5.5.2.3 Pump .....	57
5.5.2.4 Generator.....	58
5.5.2.5 Orifice Plate and Manometer .....	59
5.5.2.6. Emission Measuring Equipment .....	60

5.5.2.7. Thermocouple Thermometer.....	61
5.5.2.8. Electric Loading System .....	62
6. RESULTS AND DISCUSSION .....	63
6.1 Catalyst Characterization Results .....	63
6.1.1. SEM Analysis Results.....	63
6.1.2. XRD Analysis Results .....	68
6.1.3. BET Analysis .....	69
6.2. NO <sub>x</sub> Conversion Rates .....	71
6.2.1. Temperature Effect .....	73
6.2.2. Engine Loading Effects.....	73
6.2.3. Blend Ratio Effects .....	74
6.2.4. Maximum Conversion Rate Recorded.....	74
6.3. Conclusion and Recommendations .....	74
6.3.1. Conclusion .....	74
6.3.2. Recommendations.....	75
REFERENCES .....	77
CURRICULUM VITAE.....	83



<b>LIST OF TABLES</b>	<b>PAGES</b>
Table 3.1. Emission Standards for a High-Duty Diesel Engine.....	17
Table 3.2. Emission Standards for a Light-Duty Diesel Engine .....	17
Table 3.3. Hydrocarbons Reductants for HC-SCR and their formulas.....	29
Table 3.4. Activity of various zeolite catalysts for HC-SCR.....	30
Table 5.1. Technical specification of PANalytical EMPYREAN XRD .....	43
Table 5.2. KELVIN 1042 technical properties .....	44
Table 5.3. Physical properties of Propanol .....	46
Table 5.4. Technical properties of RADWAG AS 220.R2.....	48
Table 5.5. Vibra-Cell V750 ultrasonic processor technical properties .....	49
Table 5.6. Memmert BASIC oven UNB 500 Specifications .....	51
Table 5.7. Arduino MEGA 2560 Specifications.....	56
Table 5.8. AKSA A2CRX08 technical properties .....	58
Table 6.1. BET analysis of cordierite and Ag-Pd-Ti catalyst .....	69



<b>LIST OF FIGURES</b>	<b>PAGES</b>
Figure 1.1. Development of emissions in the European zone from transport.....	2
Figure 2.1. The four cycles combustion of a diesel engine.....	6
Figure 2.2. Various transport emissions .....	9
Figure 2.3. CO <sub>2</sub> emissions in various sectors .....	10
Figure 2.4. Sources of NO <sub>x</sub> emission.....	13
Figure 3.1. Global Emission Legislation by World Region.....	15
Figure 3.2. Emission Limits and Phase-in Timing in the different world regions .....	16
Figure 3.3. Working mechanism of an EGR.....	18
Figure 3.4. Effects of EGR .....	19
Figure 3.5. Diesel Particulate Filter .....	20
Figure 3.6. Structure of a TWC .....	22
Figure 3.7. Conversion Efficiency of TWC.....	23
Figure 3.8. Working DOC .....	24
Figure 3.9. Working of SCR.....	26
Figure 5.1. Monolith honeycomb Cordierite .....	40
Figure 5.2. Silver, Copper and distilled water .....	41
Figure 5.3. The PANalytical EMPYREAN XRD.....	42
Figure 5.4. KELVIN 1042 .....	44
Figure 5.5. FEI Quanta 650 Field Emission SEM .....	45
Figure 5.6. RADWAG AS 220 .R2 .....	48
Figure 5.7. Vibra-Cell V750 ultrasonic processor .....	50
Figure 5.8. Protherm Furnace Model PLF 110/6.....	50
Figure 5.9. Oven Cross-sectional drawings .....	51
Figure 5.10. Exhaust pipe showing the NO <sub>x</sub> sensors and the K-type thermocouple .....	54
Figure 5.11. Layout of the experiment .....	54



Figure 512 . Continental NO <sub>x</sub> sensors.....	56
Figure 513 . Arduino MEGA 2560.....	57
Figure 514 . A pump connected to an Arduino.....	57
Figure 515 . AKSA generator.....	59
Figure 5.16. Manometer with an orifice plate.....	60
Figure 5.17. MRU DELTA 1600-V.....	61
Figure 5.18. KJTRSE thermocouple thermometer logger 9682 .....	62
Figure 519 . Electric loading system .....	62
Figure 6.1. SEM images of the cordierite.....	64
Figure 6.2. SEM images of the prepared catalyst.....	65
Figure 6.3. Mapping images of the catalyst.....	67
Figure 6.4. XRD results of the cordierite.....	68
Figure 6.5. XRD results of the catalyst.....	69
Figure 6.6. Cordierite BET plot.....	70
Figure 6.7. Catalyst BET plo .....	70
Figure 6.8. NO <sub>x</sub> conversion rate at 30000h <sup>-1</sup> /1-4 KW/ Propanol %100.....	71
Figure 6.9. NO <sub>x</sub> conversion rate at 30000h <sup>-1</sup> /1-4 KW/ Propanol %95 - Adblue%5.....	72
Figure 6.10. NO <sub>x</sub> conversion rate at 30000h <sup>-1</sup> /1-4 KW/ Propanol %90 - Adblue%10.....	72

## LIST OF ABBREVIATIONS AND NOMENCLATURE

C	:	Celsius
Ag	:	Silver
F	:	Fahrenheit
Pd	:	Palladium
KW	:	Kilowatt
XRD	:	X-ray Diffraction
XRF	:	X-ray Fluorescence
BET	:	Brauner– Emmett – Teller
DOC	:	Diesel oxidation catalyst
SCR	:	Selective catalytic reduction
NO <sub>x</sub>	:	Oxides of Nitrogen
SO <sub>x</sub>	:	Sulfur Oxides
PM	:	Particulate matter
CO	:	Carbon monoxide
EGR	:	Exhaust gas recirculation
DPF	:	Diesel particulate filter
TWC	:	Three-way catalytic converter
SV	:	Space Velocity



**1. INTRODUCTION**

Climate change indicates an enormous range of global phenomena occurred primarily by burning fossil fuels which heat-increasing gases to the atmosphere. The increased temperature trend is defined as global warming, but also changing of sea levels, ice mass loss in the North pole, shifting in flower and animal range and extraordinary weather events (Anonymous 1).

The international problems caused by human which effected the sphere is one of the major critical topics for nature. Because of this situation, Earth calls out rising acidification of the deep and more than 1 cm of water level scale-up and drought have affected food chains all around the world (Levitus, 2012; Meyssignac 2012).

If these activities will not be prevented and controlled, it is expected that the global climate will chop about and there will be some negative effects on the world. (Huddleston, 2012).

The continuum of the greenhouse gas effect during which radiation from the solar is trapped within aureola, which warms the earth. The natural greenhouse effect is being changed by human activities on Earth (Anonymous 2). There are some factors to affect greenhouse gas emissions such as agriculture, industry, electricity production increase the concentration of unwanted gases (Anonymous 3).

Emissions of these unwanted gases affect health and the environment. The content of these harmful gases includes respectively; 72.1% carbon dioxide (CO<sub>2</sub>), 18.3% methane and 9.2% nitrous oxide (NO<sub>x</sub>). Except for this, the major reason for worldwide warming is harmful carbon dioxide emissions. This is comprised of some factors such as the burning of fuels, like ethanol, petrol. Emissions of CO<sub>2</sub> have been sharply accrewed for fifty years and are enhancing nearly 3.01% per year (Anonymous 4).

Emission of greenhouse gases increased at a faster rate over the first decade in the 21st century than they did over the past three decades and it reached the peak level in human history (Anonymous 5).

The transportation industry is both a great subscriber to the worldwide economy and the cause of climate change and environmental pollution. Specifically, motor vehicles cause 22% of all global CO<sub>2</sub> emissions (IEE, 2012). Figure 1.1 shows the development of emission levels from transport.

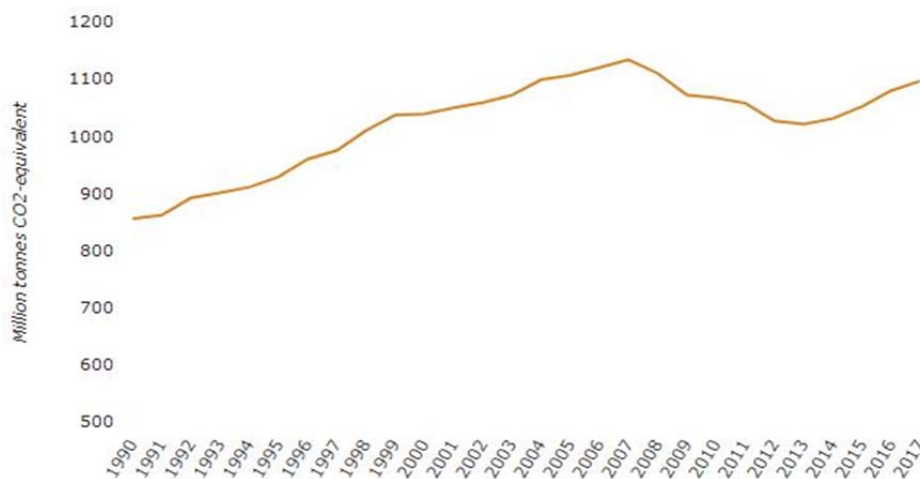


Figure 1.1. Development of emissions in the European zone from transport (Anonymous 6)

Transportation is a noteworthy and substantial subscriber to air contamination. Calculated responsibility of 30% of particulate emissions (PM) is occurred by road transport and because of traffic complication, this proportion may scale up to 50% in OECD countries. Nevertheless, the sum part of transport to particulate weather complications can considerably, from 12.1% to 70% of the sum dirtiness mixture. Less developed and underdeveloped countries suffer from transport based contamination. Old, effete diesel cars, trucks and for want of public transportation engines are the major problem of air contamination (Anonymous 7)

Diesel engines are the primary requirements because they are widespread operated in many areas including transportation goods, people, services. They are the ones for buses, trains, ships, and so many vehicles.

The fields to be used diesel engines are growing fast all around worldwide. Because a diesel engine has better efficiency and reliability. Nevertheless, there are some disadvantages. Some of them are the biggest contributors to contamination problems all around the world with big raises expected in engine inhabitants causing ever-increasing global emissions of DPM (diesel particulate materials) and NO<sub>x</sub> (Xia, 2015).

The information elaborated above, scientists have been busy with researches and experiments to develop the NO<sub>x</sub> reduction technologies in the automotive sector. These purposes are getting difficult to catch ever-evolving emission standards.



## 2. DIESEL ENGINES AND EMISSIONS

### 2.1 Diesel Engines

Otto first improved the gasoline engine in 1876 when date back to internal combustion engine history and then Rudolf Diesel devised the diesel engine in 1892 (Anonymous 8).

The main divergence among two model engines is in the ignition of the fuel. The ignition in the Otto engine is taken place by the spark caused by a spark plug, this is the main reason why it is known as the spark-ignition engine. Conversely, the ignition in the compression ignition engine is made by compressing the combustible, it is the main reason why it is known as a compression-ignition engine (Anonymous 9). Diesel engines work with extreme air because upward of air is behooved to perfect combustion of the combustible. The hydrocarbon and particulate matter are reduced as excess air increases because of this is an environmental advantage. Due to extra air, diesel engine exhaust involves a high amount of oxygen, extra oxygen avoids higher exhaust gas and because of this reason, diesel engines have a lower CO<sub>2</sub> footprint compared to gasoline engines (Sitshebo, 2010). Generally, diesel engines can be categorized into two categories according to the number of crankshaft revolutions per working cycle. Two-stroke and four strokes belong to these two categories. Stroke is defined as full distance travel by the piston in a one-way destination. Only in an upward and downward way is it allowed for the piston. To achieve the four-piston cycle in four-stroke engines, the piston must take out two times up and down, besides the crankshaft has to pull away two full revolutions. In most, both two types of engines (light and heavy) conduct on a four-stroke cycle, these are a suction stroke, a compression stroke, expansion stroke, and exhaust stroke (Anonymous 10). Firstly, Fresh air enters into to cylinder when the piston moves down the chamber with the intake valve open in the induction stroke. At the end of this stroke, the piston moves to the bottom dead center. But the exhaust valve remains to inclose along



the period. In compression stroke, the piston upsurges from the bottom dead center to top dead center and during this period intake and exhaust valves are closed when fresh weather is jammed. Because of these movements, great pressure and temperature enhanced inside the cylinder. At the end of the compression stroke when the piston is at the top end of the cylinder a metered quantity of diesel is injected into the cylinder by the injector. The heat of compressed air ignites the diesel fuel and generates high pressure which pushes down the piston in power stroke. When the piston reaches the bottom end of the cylinder after the power stroke, the exhaust valve opens while the inlet and fuel valve is closed. The pressure in the cylinder is higher than atmospheric pressure because of the burned gases inside the cylinder. This pressure difference allows burnt gases to escape through the exhaust port and the piston move through the top end of the cylinder. At the end of an exhaust stroke, the exhaust valve closes and the cycle is thus completed (Sitshebo, 2010; Anonymous 11). The typical heavy-duty and light-duty diesel engine's combustion process is exhibited in Figure 2.1.

#### Four-stroke cycle (Diesel)

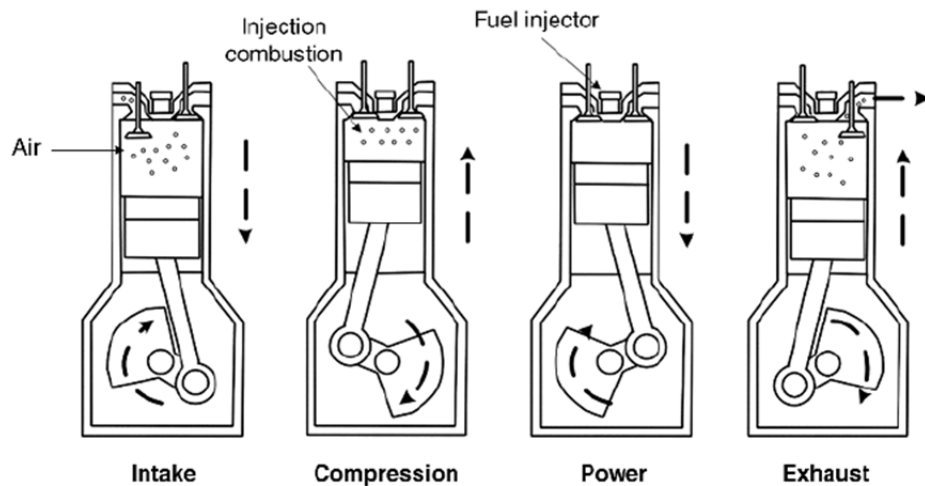


Figure 2.1. The four cycles combustion of a diesel engine (Anonymous 12)

Exhaust gas emissions of diesel engines are affected by some factors such as combustible delivery system, fuel submittal piezo (Sitshebo, 2010).

## 2.2 Emissions from Diesel Engines

Normally, in diesel combustion process must emit only  $\text{CO}_2$  and  $\text{H}_2\text{O}$  because exhaust with carbon oxidized to  $\text{CO}_2$  and hydrogen to  $\text{H}_2\text{O}$  (Anonymous 13). Besides, as the oxidation reaction continues, the glowing continuum generates  $\text{CO}_2$ ,  $\text{H}_2\text{O}$ , and  $\text{H}_2$  on the other hand pollutants that mean undesirable products are formed also. Generally, pollutants can be categorized into 3 groups which are solid (particulate matters), unburned hydrocarbons (liquids) and gas matters (Wang, 2014).

After this point, emission varieties and their hazardous impact will be elaborated which caused by incomplete combustion, unburned fuels and insufficient temperatures.

### 2.2.1 Sulfur Oxides ( $\text{SO}_x$ )

Sulfur dioxide ( $\text{SO}_2$ ) is made from the sulfur compounds in the compression ignition combustible (Anonymous 14). Fundamentally, a sulfur oxide is spread when the fuel or other materials involving sulfur are combusted or oxidized. The emission of  $\text{SO}_2$  in the exhaust gas hinge on the sulfur context of the fuel (Anonymous 15). The sulfur oxide is known as a pollutant due to its role and effect which along with particulate matter, informing winter-time smog causes serious weather contamination in point of its opposing effect on the health of organisms. Recent workings have shown that  $\text{SO}_2$  stirs up tantrum stimulation in the lining of the nose and throat (Anonymous 16). There are some factors to reduce  $\text{SO}_2$  emissions such as; fulfilling the national fuel quality standards, specifying tighter vehicle emission standards and supporting alternative fuels (Anonymous 17).

### 2.2.2 Particulate Matter (PM)

It is identified as the piles of little corpuscle by virtue of the combustion continuum because of partially lighted oils, a cinder quantity of the combustible applied by the engine of the vehicles, sulfates from the engine cylinder wall lubrication oil and water from condensation and the combustion process. Emissions of heavy-duty engines are categorized as 41.1% as carbon, 7.2% as combustible (but not fully burned), 25% as an oil (but not fully burned), 14% as sulfates and water, and 13% as ash and various components emissions due to experimental work. Another study shows that those emissions of particulate matter arose from  $\cong 29.9\%$  elemental carbon,  $\cong 13.9\%$  sulfates and damp,  $\cong 7.99\%$  combustible (but not fully lighted), and  $\cong 39.9\%$  unburnt lubricating oil (Anonymous 18).

Particulate matter emissions can be categorized into three essential groups named soot, soluble organic fraction and the inorganic fraction. Above %49.9 of emissions of particulate matter come from ash. It can be observed as black smoke. When exhaust temperatures are not high levels, SOF worths are getting great at not high engine burdens. PM emissions formation is managed in several ways, for instance, quality of fuel, exhaust gas cooling system (Anonymous 18).

Particulate Matter (PM) is an exhaust emission of compression ignition engines that has a greater rate compared with the emission of spark ignition (SI) engines. The unsuitable blast continuum in the cylinder is caused by this difference. When the engine load increases, PM concentration rises in line. High combustion temperature can minimize the formation of particulate matter, however, considerable great combustible concentration in an engine produces particulate matter emissions under the engine conditions. PM can cause considerably wellness problems such as hard breathing, asthma (Tira, 2013).

### 2.2.3 Carbon Dioxide (CO<sub>2</sub>)

It is mostly harmless gas and also it has some positive properties such as being colorless and odorless. However, it has some negative properties such as sharp acidic odor at high concentrations and it pretends as an irritant and asphyxiant (Sitshebo, 2010).

As a result of higher combustion and volumetric efficiencies, compression ignition engines generate lower CO<sub>2</sub> emissions each kilometer comparison with spark-ignition engines. According to a European Commission report, in various sectors like industry and automotive companies carbon dioxide emission is being reduced but in the transportation sector, CO<sub>2</sub> emission has raised sharply from the 1990s (Figure 2.2). If this growing proportion is kept going, CO<sub>2</sub> in the transport sector will surpass all the other sectors combined to become the primary source of greenhouse gases by 2050 (Figure 2.3) (Wang, 2014).

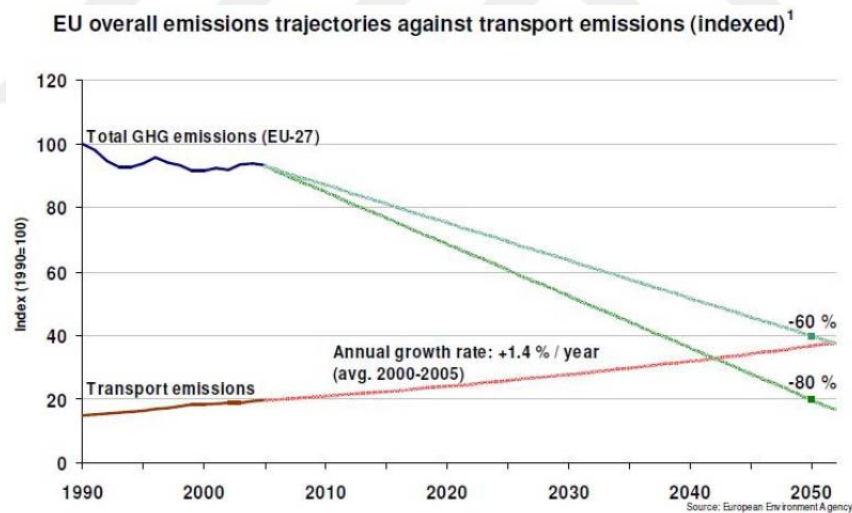
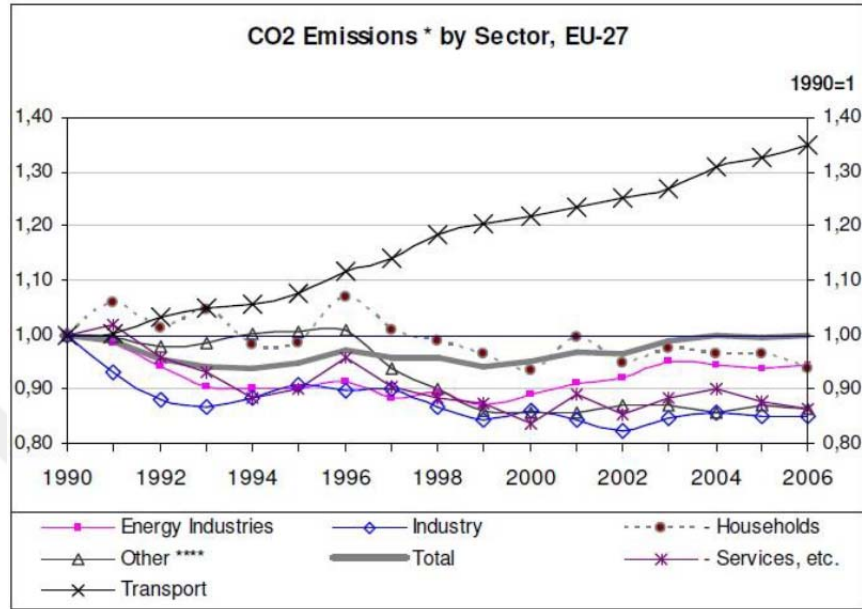
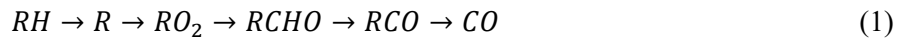


Figure 2.2. Various transport emissions (Wang, 2014)

Carbon dioxide emissions by sector EU-27 (indexed)<sup>2</sup>Figure 2.3. CO<sub>2</sub> emissions in various sectors (Wang, 2014)

### 2.2.4 Carbon Monoxide (CO)

It is a colorless and non-corrosive gas formed by imperfect combustion. Because of the lack of oxidants, temperature and residence time while the combustion continuum, CO formation is increased. CO formation is a product formed by imperfect combustion, HC based fuel and it can be summed up as noted below with R signifying the HC radical (Sitshebo, 2010).



If the whole fuel is burned complete combustion is formed in the exhaust gas so there will be zero parts of unburnt combustible. If the air-fuel ratio is higher than 1, it is known as a lean and if the air-fuel ratio is lower than 1, it is known as a rich mixture (Anonymous 19).

In general, the rich blends generate the greatest yields of CO because of the deprivation of the oxidant. Due to the high amount of air in diesel operation, CO emission is lower than gasoline engines and the oxidation equation CO to CO<sub>2</sub> is shown below (Sitshebo, 2010).



There are some ways to form and accelerate CO emission such as heavy concentrated traffic, parking garages. A combination of these matters causes a heart attack (Tira, 2013).

### 2.2.5 Hydrocarbons (HC)

It is a chemical composite matters include hydrogen and carbon. Significant numbers of engines, buses, midibuses are run by using essential hydrocarbon-based combustible such as gasoline and diesel (Anonymous 20).

HC emissions formation are affected in a number of ways. Because of misfiring and lean mixing, the temperature in the cylinder is reduced by greater warmth caliber and deprivation of oxygen in the combustion chamber so it representing in slower combustion rate allowing the unburnt blend to break up the blast chamber (Tira, 2013).

Basically, HC is formed by incomplete combustion and unburnt fuels as a result of insufficient temperature (Anonymous 21).

There are some methods to reduce HC emissions by rising fuel injection piezo. High concentrate emission can give a cycling changefulness as a result of partial burning or undesirable firing periods (Tira, 2013).

There are particularly negative environmental and human health effects because of HC emissions and also, they are primarily responsible for the formation of ground-level ozone. 50% of the form of ozone emissions are caused by vehicles, HCs are poisonous and might stir up death (Resitoglu, 2015; Anonymous 22).

**2.2.6 Oxides of Nitrogen (NO<sub>x</sub>)**

Both NO and NO<sub>2</sub> produce nitrogen oxides with the former being the amplest and forming more than 70-90 % of the whole NO<sub>x</sub>. There are several factors to affect the formation of NO<sub>x</sub> such as high temperatures and pressures due to diesel engine combustion properties. The key source is atmospheric nitrogen for the formation of NO<sub>x</sub>.



At an ordinary flame temperature, NO<sub>2</sub> /NO ratios should be lower enough to proceed with chemical equilibrium. However, this ratio is higher in diesel engines and corresponds to almost %30 of the total oxides and this situation causes NO<sub>2</sub> emission so the formation of NO<sub>2</sub> is shown below equations.



The following equation represents what happens when decay occurs:



At low load, the formation of NO<sub>2</sub> is accurate then resulting in lower combustion temperatures and hindering NO<sub>2</sub> decomposition (Sisthebo, 2010). Mainly, road transport is an essential effect to cause NO<sub>x</sub> emissions which constitute 40–70 % of the NO<sub>x</sub> by self. Although there are different types of

vehicles, diesel vehicles are the greatest valuable contributors to  $\text{NO}_x$  emissions. Diesel engines need greater heats in comparison to gasoline engines since diesel engines are compression-ignition engines and they account for above 85 % of all the  $\text{NO}_x$  emissions from mobile sources (Resitoglu, 2015). Figure 2.4 shows the sources of  $\text{NO}_x$  emission.

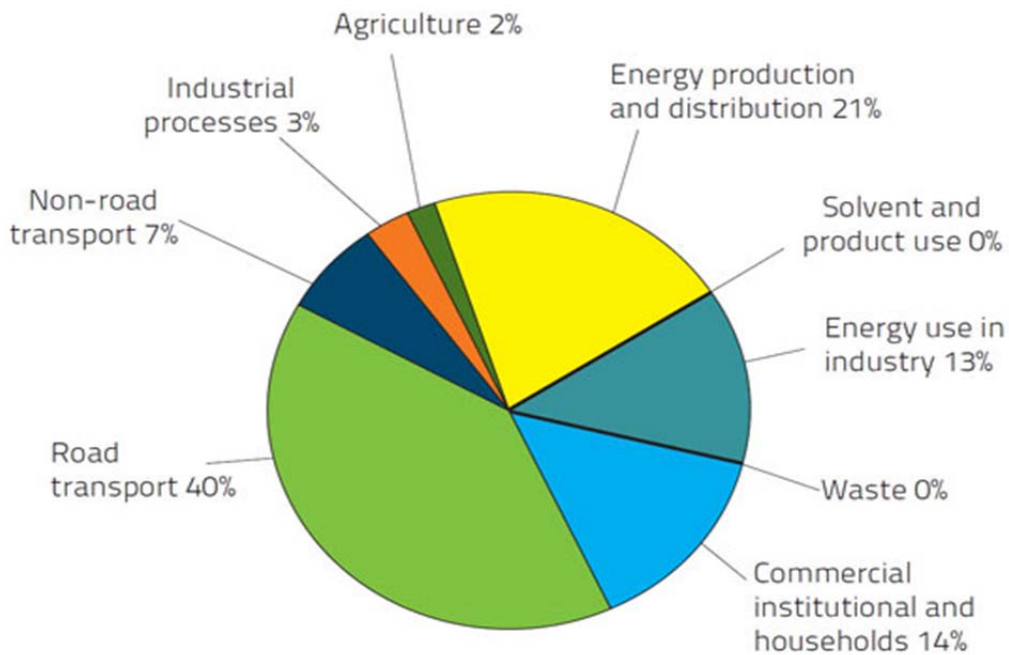


Figure 2.4. Sources of  $\text{NO}_x$  emission (Anonymous 23)

There are some paths to cut down on the detrimental impacts of  $\text{NO}_x$  emissions by reducing combustion temperature through the steam, decreasing the residence time at the great cylinder temperature through the ignition, using after-treatment systems like SCR (Tira, 2013).

$\text{NO}_x$  emission has negative properties. Drawing this emission and its oxides cause poisonous side effects by provoking both lung infection and respiratory allergies. Also, it influences the formation of acid rain, ground-level ozone (Wang, 2014).





### 3. EMISSIONS REGULATION AND MINIMIZATION

#### 3.1 Emissions Regulations

There are different emission regulations types in the world. Many countries in the world have own regulations and emission standards. For example, European countries use Euro standards, America uses Tier standards, India uses Bharat standards, China uses China standards (Anonymous 24). Vehicle standards of some countries and emission limit levels are shown below figures.

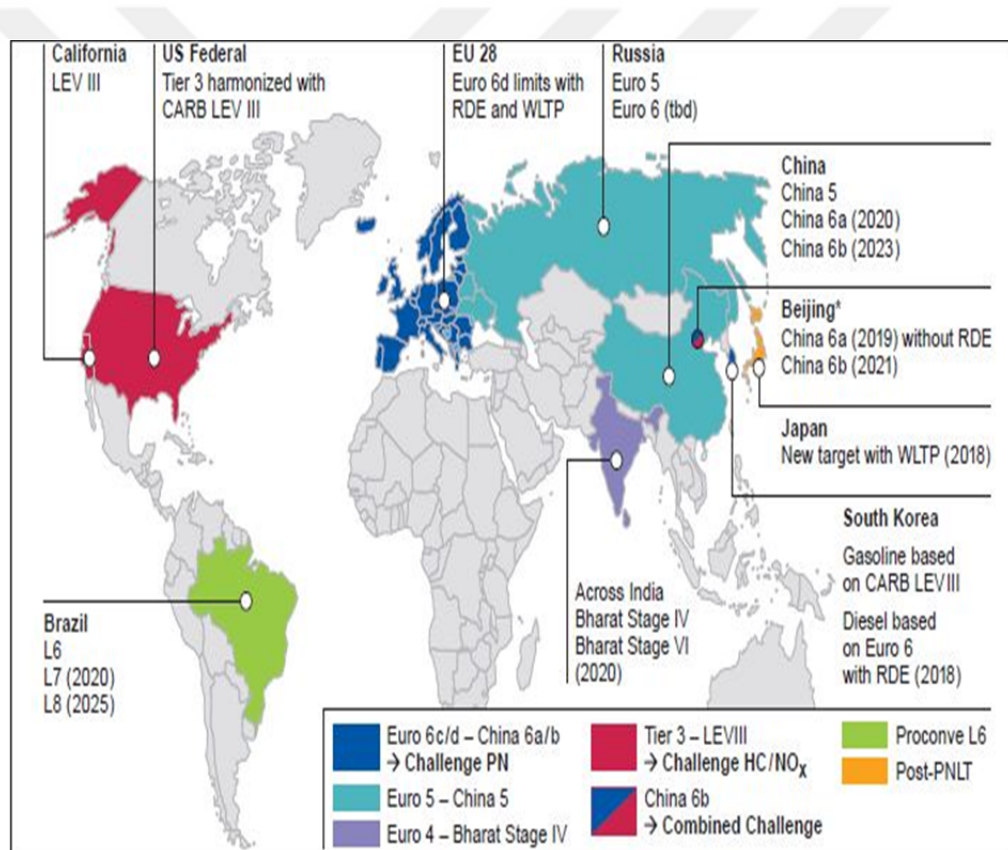


Figure 3.1. Global Emission Legislation by World Region (Anonymous 25)

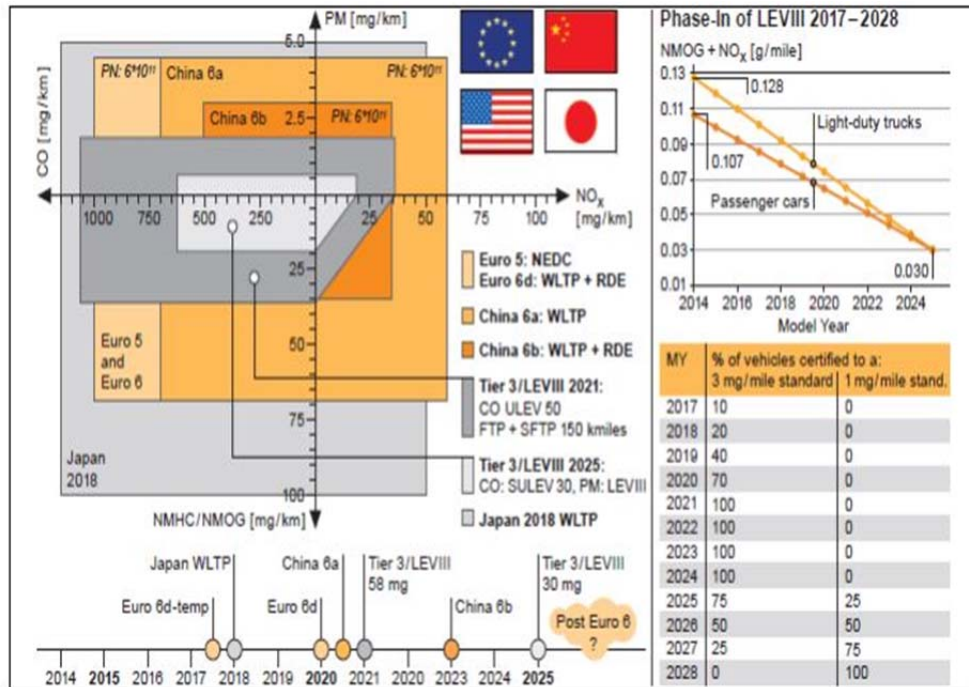


Figure 3.2. Emission Limits and Phase-in Timing in the different world regions (Anonymous 25)

The first emission standards of vehicles came in 1988. In our country, Euro Standards are used as emission standards. European emission standards are the most common and most important legislation in the world (Anonymous 26). The aim of these standards is to protect and enhance air quality, decrease greenhouse gas emission and air pollution (Anonymous 27). Euro standards are updated every few years. There are limitations to decrease carbon monoxide, hydrocarbons, nitrogen oxides and diesel particulate matter (PM) by virtue of this Euro standard (Anonymous 28). European Emission standards steps for both vehicles(heavy and light) are shown below tables.

### 3. EMISSIONS REGULATION AND MINIMIZATION Osman Cenk CANDEMİR

Table 3.1. Emission Standards for a High-Duty Diesel Engine (Anonymous 26)

	CO (g/kWh)	HC+NO <sub>x</sub> (g/kWh)	NO <sub>x</sub> (g/kWh)	PM (g/kWh)
Euro I	3,16	1,13	-	0,18
Euro II	1	0,7	-	0,08
Euro III	0,64	0,56	0,50	0,05
Euro IV	0,50	0,30	0,25	0,025
Euro V	0,5	0,230	0,180	0,005
Euro VI	0,5	0,170	0,080	0,005

Table 3.2. Emission Standards for a Light-Duty Diesel Engine (Anonymous 29)

	CO (g/kWh)	HC+NO <sub>x</sub> (g/kWh)	NO <sub>x</sub> (g/kWh)	PM (g/kWh)
Euro I	3,16	1,13	-	0,18
Euro II	1	0,7	-	0,08
Euro III	0,64	0,56	0,50	0,05
Euro IV	0,50	0,30	0,25	0,025
Euro V	0,5	0,230	0,180	0,005
Euro VI	0,5	0,170	0,080	0,005

Studies have been focused to find out new redresses to decrease emissions and air pollution and increase air quality by using some different techniques, such as exhaust gas recirculation (EGR), diesel oxidation catalyst (DOC), three-way catalytic converter (TWC), diesel particulate filter (DPF) and the selective catalytic reduction (SCR) technique. Each technique has very important and characteristic properties to prevent and minimize pollutant emissions. For example, EGR is applied to cushion emissions of NO<sub>x</sub> whereas DOC is used to decrease CO and HC. DPF is the main technique to reduce PM emissions. Three-way catalytic (TWC)

converters are applied to check  $\text{NO}_x$ , HC and CO emissions. For the reduction of  $\text{NO}_x$ , the most effective and important method is SCR. Three-way catalytic (TWC) converters are used to control  $\text{NO}_x$ , HC and CO emissions (Anonymous 18).

### 3.2 Emissions Control Systems

These various techniques will be illustrated in the next part. Especially, DOC, DPF, TWC and SCR systems are focused due to the fact prevalent usage in heavy-duty vehicles.

#### 3.2.1 Exhaust Gas Recirculation (EGR)

It is the most known method to cushion  $\text{NO}_x$ . It is primarily used to control and decrease the  $\text{NO}_x$  content of the exhaust gas. Because of its simplicity and low-cost implementation, it is a highly desirable technique, so this method is prevalently used in most diesel engines. The utilization of EGR is easy and popular. The application of EGR is the recirculation of exhaust gas back into the combustion chamber by mixing it in with the weather charge (Anonymous 30). The schematic of the working mechanism of an EGR is shown below figure.

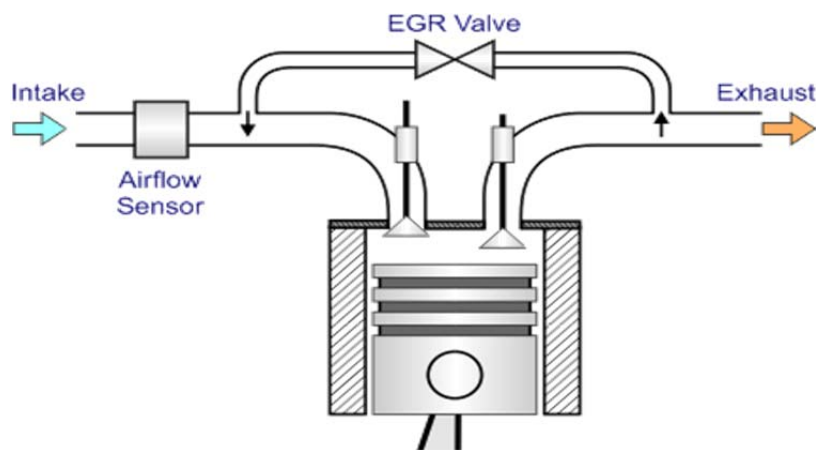


Figure 3.3. Working mechanism of an EGR (Anonymous 31)

### 3. EMISSIONS REGULATION AND MINIMIZATION Osman Cenk CANDEMİR

So, combustion efficiency and temperature decrease due to entering fresh air and NO<sub>x</sub> emissions are reduced. Also, engine life is better and improved due to reducing combustion temperature. But there are some disadvantages because lower NO<sub>x</sub> and low combustion temperature mean increasing in HC, CO and PM emission, so to comply with strict emissions regulations, more effective control systems must be used (Anonymous 18). The effects of EGR are shown below figure.

Effect of EGR	Effective EGR components	Main influence of the effective components	Effect on NO <sub>x</sub>	Effect on PM
Dilution	O <sub>2</sub>	Restricted O <sub>2</sub> concentration	80 – 90 % reduction	80 – 90% increase
Chemical	CO <sub>2</sub>	Thermal dissociation and participation in the combustion	5 – 10 % reduction	5 – 10 % reduction
	H <sub>2</sub> O			5 – 10 % increase
Thermal	CO <sub>2</sub>	Acting as heat absorbers due to high specific heat capacity	Less than 5 % reduction	Small
	H <sub>2</sub> O			
Inlet Temperature (Hot EGR)	NA	Increased inlet charge temperature and reduced volumetric efficiency	Increase (proportional to inlet charge temperature)	Increase (proportional to inlet charge temperature)

Figure 3.4. Effects of EGR (Wang, 2014)

#### 3.2.2 Diesel Particulate Filters

DPF has been used in production in the buses, midibuses, vehicles since 2000. It is primarily used for reducing PM emission (Anonymous 18).

Exhaust gas is acutely moved from beginning to end the walls, aggregating the soot particles within the leachier wall and over the inlet channel surfaces to filter PM. So it has two-sided advantages for decreasing the mass and number of the emitted particles (Wang, 2014). The schematic working of DPF is shown below figure.

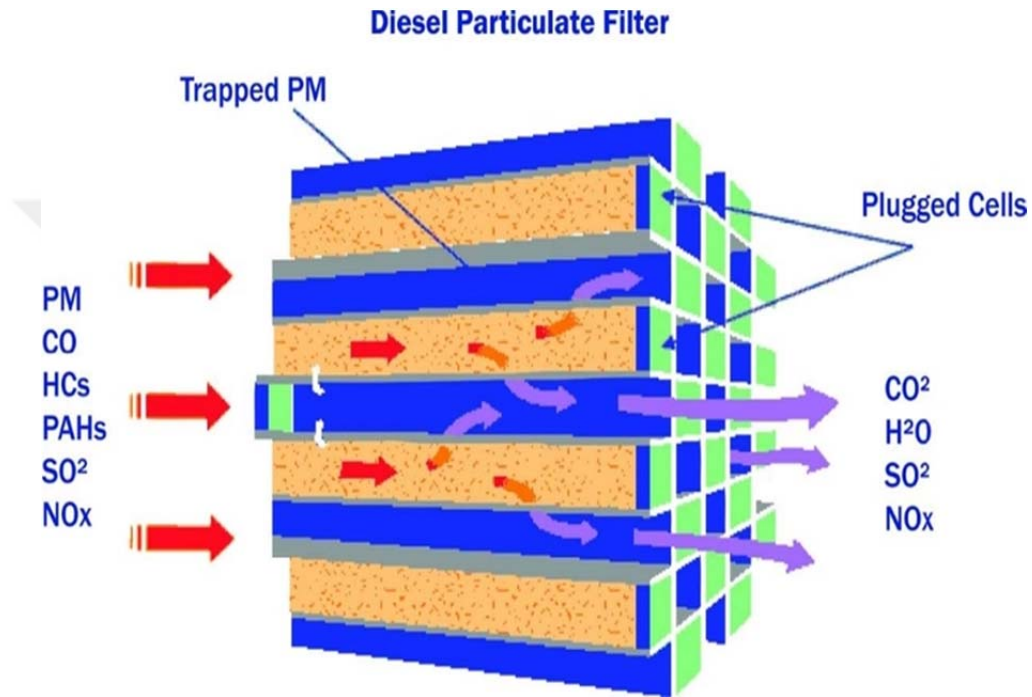


Figure 3.5. Diesel Particulate Filter (Anonymous 32)

Because of accumulating soot in a filter, it occurs back pressure and it leads to a negative effect on engine fuel economy by increasing fuel consumption. The collected soot must be burnt, and this process is called regeneration. The regeneration process is used for this circumstance to remove the soot, accumulating in the filter (Wang, 2014).

There are two types of regeneration: active and passive regeneration. In passive regeneration, the accumulated soot in the DPF is burnt by the heat occurred by the engine during driving. This operation comes true without driver intervention (Anonymous 33). In other words, passive regeneration occurs automatically when

the exhaust temperature is high. Most of the vehicles don't get this kind of use though so manufacturers must design-in active regeneration where the engine management computer (ECU) takes control of the process (Anonymous 34).

In active one, the temperature of the exhaust gases is increased, and more fuel is injected, and diesel particulates are oxidized. In comparison with passive regeneration, active regeneration has a higher operating cost (Anonymous 33).

### **3.2.3 Three-Way Catalytic Converter (TWC)**

It is applied to check NO<sub>x</sub>, HC and CO emissions. Special catalysts are used to decrease NO<sub>x</sub> and oxidize HC and CO in the same timeline and because of that reason, it is known as three because it impairs three important gas emissions. These special catalysts contain platinum, palladium, and rhodium that means they are used as an oxidation catalyst (Anonymous 35). The structure of the TWC is shown in Figure 3.6.



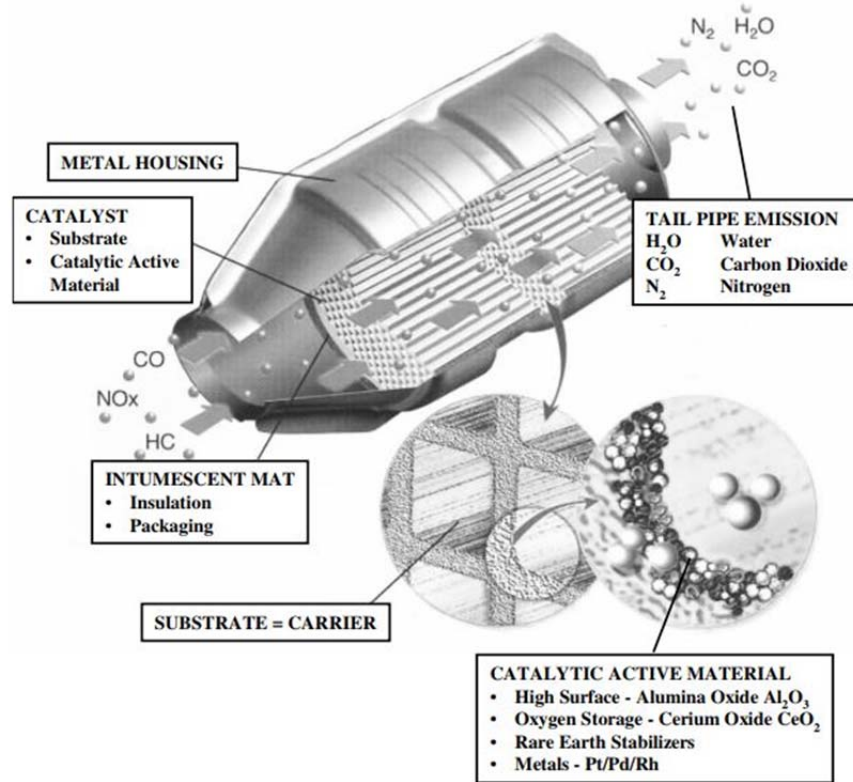


Figure 3.6. Structure of a TWC (Anonymous 36)

The characteristic of the fuel mixture is important for the conversion efficiency of TWC. As the nitrogen oxides conversion falls significantly at lean fuel mixtures, CO and HC increase slowly. This situation is reversed compared to the lean mixture (Anonymous 37) Figure 3.7 illustrates the situation.

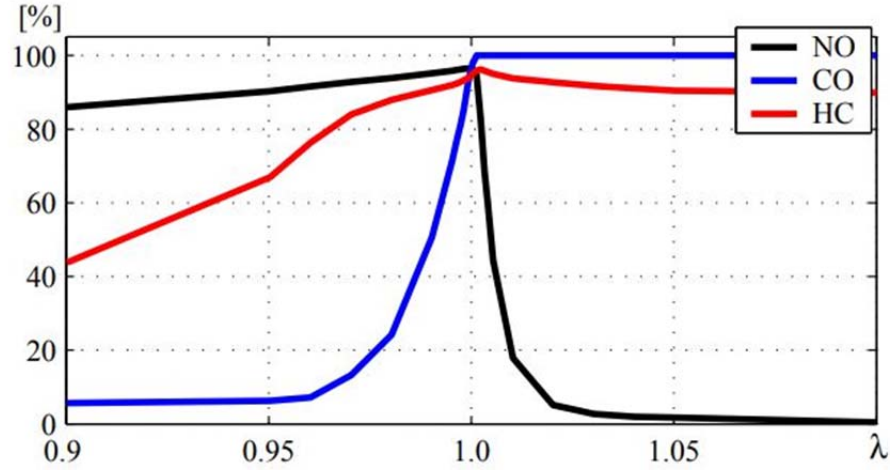
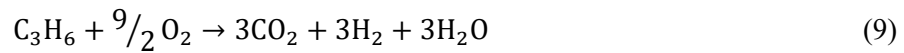


Figure 3.7. Conversion Efficiency of TWC (Anonymous 36)

### 3.2.4 Diesel Oxidation Catalyst

Primarily objective of DOCs is to oxidize HC and CO emissions (Anonymous 18). DOC has also another important mission. It is used associated with the SCR catalyst to oxidize NO into NO<sub>2</sub> so NO<sub>2</sub>/NO<sub>x</sub> ratio increases and this leads to a decrease of NO<sub>x</sub>. The efficiency of DPF and SCR is increased due to a higher NO<sub>2</sub> concentration in the NO<sub>x</sub> (Resitoglu, 2015). There are three main reactions happening in DOCs which are shown in Equations in 8, 9 and 10.



### 3. EMISSIONS REGULATION AND MINIMIZATION Osman Cenk CANDEMİR

The efficiency of DOC depends on various parameters such as reactive surface, catalyst load and temperature. The most critical parameter is temperature. At high exhaust temperatures, DOC can procure better checks of HC and CO emissions with reduction efficiencies greater than 90% (Anonymous 38). The working schematic of DOCs is shown below figure.

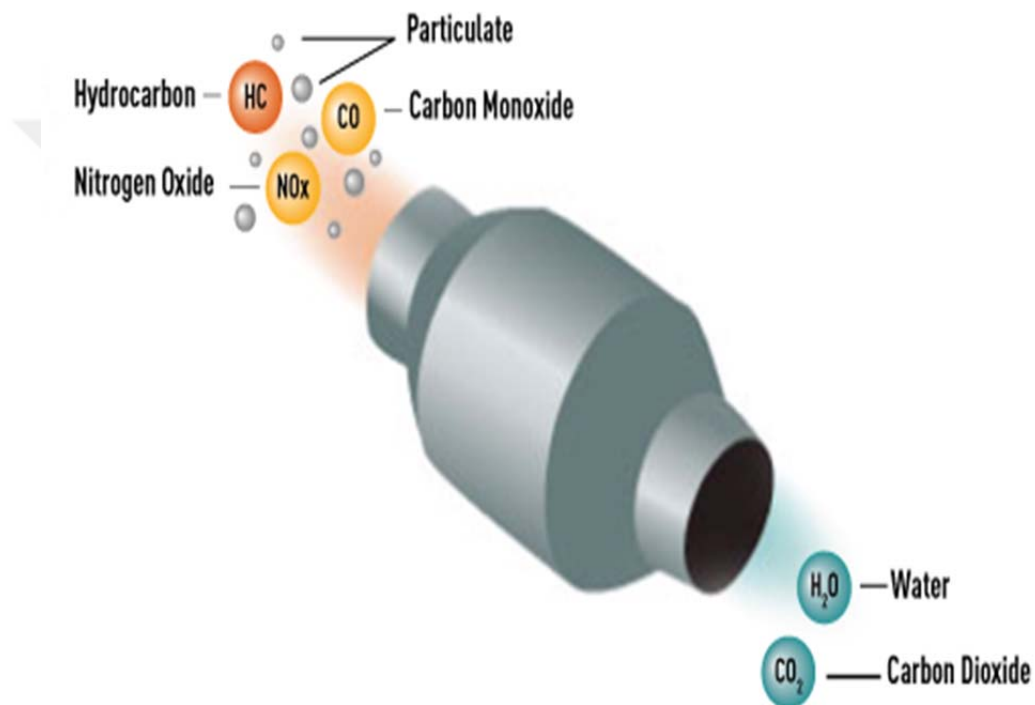


Figure 3.8. Working DOC (Anonymous 39)

### 3.2.5 Selective Catalytic Reduction

SCR was found in 1957 patented by the Englehard Corporation. SCR catalyst which contained vanadia was the first useful application that developed in Japan. Today, SCR systems are used in many different areas comprising industrial boilers, turbines, automotive, furnaces, coke ovens (King, 2003).

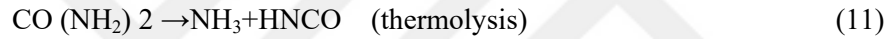
SCR is the most effective and common technique to reduce  $\text{NO}_x$  emissions. It is better for improved for high duty vehicles compared to light-duty vehicles because of the low exhaust temperature of light-duty engines. But there has been a huge improvement in light-duty vehicles, many manufacturers like Mercedes, Nissan, Audi have been using this technique in their vehicles.  $\text{NO}_x$  emissions in the exhaust gas are minimized in the SCR system by using different types of reductant such as HC, ammonia, and urea (Resitoglu, 2015).

Ammonia was the first reductant used as a reducing agent in the SCR systems but there are many problems with using ammonia because of mainly safety reasons. Ammonia is very harmful to humans, animals, and the environment because it is very corrosive, flammable, toxic and hazardous. Furthermore, it is hard to store and on-board transport safely because of its high vapor pressure and to prohibit these problems, ammonia is chemically transformed into urea. Urea is used as a reductant in SCR because it has odorless, nonpoisonous and nonhazardous properties (King, 2003). Urea is a compound of 32.5% urea and 67.5% water. It is sold commercially under the name AdBlue. Because of its high water ratio in the urea solution, it has a low freezing point (Müller, 2003). The principle of SCR is shown below figure.

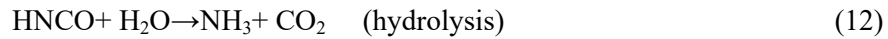


Figure 3.9. Working of SCR (Müller, 2013)

There are two processes namely hydrolysis and thermolysis to urea decomposes into ammonia. First, urea decomposes into isocyanic acid and ammonia as shown in reaction 11.



Next, isocyanic acid and water react by hydrolysis to form another ammonia molecule as shown in reaction 12.



After these two processes, the below reactions are taking place in the SCR catalyst (Anonymous 18).



The ideal working range of the SCR system is between 200.1°C and 600.2°C. Counterchecks start mostly at higher than 199°C and most desirable and the highest efficiency is achieved at 350°C. If the reaction temperature is lower than 200°C, there will be some undesirable conditions such as cyanide acid, melamine. These compounds have negative effects to process due to they could collapse in the exhaust pipe and cylinder wall (Resitoglu, 2015).

Owing to better selectivity and reactivity, urea has been evaluated as the most important reductant for the SCR. But there are some drawbacks to using Urea-SCR. The most important thing is the amount of injected urea must be precise to remain the great transformation of NO<sub>x</sub> (Sawatmongkhon, 2011).

#### **3.2.5.1 Hyrdocarbons SCR (HC-SCR)**

Hydrocarbons can be used as a reductant instead of urea because of several reasons. Lower exhaust heat is a big situation for this type of SCR because when the exhaust temperature is lower than 200°C, the reactions in the urea can't occur properly. So, the efficiency of the transformation of nitrogen oxides of urea- SCR is restricted at low heat (Sawatmongkhon, 2011).

On the other hand, The certain positive effects of HC-SCR is that the on-board fuel can be used as a reductant for NO<sub>x</sub> conversion, which reduces the cost involved in the development of infrastructure for delivering reductant to an automotive engine exhaust system. And also, existing of HC in the exhaust gas and eliminating the urea tank are the other advantages compared to urea-scr (Resitoglu, 2017).

#### **3.2.5.2 Reductants for HC-SCR**

Various types of hydrocarbons have been used in the SCR system as can be seen in Table 3.1. Some of them are lower hydrocarbons (C<sub>1</sub> – C<sub>4</sub>), higher hydrocarbons (>C<sub>6</sub>), diesel fuel and alcohol. The efficiency of conversion of NO<sub>x</sub>

to  $N_2$  by hydrocarbons is alkanes < alkenes < oxygenated, respectively (Hyuk, 2004).

Hong He et al shows that a high level of conversions of  $NO_x$  related to C content. They demonstrated that the efficiency order of the reductants for the SCR of  $NO_x$  over  $Ag/Al_2O_3$  is proposed as follows:  $C_4 > C_3 > C_2 > C_1$ . The reductants used in their experiments were classified as: C ( $CH_3OH$ , dimethyl ether (DME)),  $C_2$  ( $C_2H_5OH$ ,  $CH_3CHO$ ),  $C_3$  ( $C_3H_6$ , isopropyl alcohol (IPA), 1-propanol and acetone) and  $C_4$  (1-butanol) (He, 2007).

Oxygenated hydrocarbons like propanol, ethanol, acetone enable great conversion efficiencies of  $NO_x$  (above 80%) at  $250^\circ C$ - $400^\circ C$ . If the alumina-supported silver catalyst is used, the conversion efficiency of  $NO_x$  is in the order of 2-propanol > acetone > ethanol > 1-propanol  $\gg$  methanol at  $350^\circ C$  (Sitshebo, 2010).

There are differences between the long-chain and short-chain alkanes. One of the most important reasons is long-chain alkanes such as diesel, show perfect improvement at low temperatures ( $200^\circ C$ ). Short-chain alkanes, alkenes, and long-chain hydrocarbon are also applied as reductants with  $Ag/Al_2O_3$  (Andreas, 2016). Some of the important hydrocarbons are shown in Table 3.3.

Table 3.3. Hydrocarbons Reductants for HC-SCR and their formulas (Guangyan, 2017)

Some of the Hydrocarbons studied as reductants	Formula
<b>Methane</b>	$CH_4$
<b>Ethane</b>	$C_2H_6$
<b>Propane</b>	$C_3H_8$
<b>n-Butane</b>	$C_4H_{10}$
<b>n-Pentane</b>	$C_5H_{12}$
<b>n-Hexane</b>	$C_6H_{14}$
<b>n-heptane</b>	$C_7H_{16}$
<b>Cyclohexane</b>	$C_6H_{12}$
<b>n-Octane</b>	$C_8H_{18}$
<b>Propene</b>	$C_3H_6$
<b>Methylcyclohexane</b>	$C_7H_{14}$
<b>Benzene</b>	$C_6H_6$
<b>Toluene</b>	$C_7H_8$
<b>Cumene</b>	$C_9H_{12}$



### 3.2.5.3 Catalysts for HC-SCR

Several kinds of catalysts have been worked to explore the HC-SCR catalyst in terms of activity, effectiveness (Gill, 2012). In 1990, Iwamoto found the first powerful catalyst for HC-SCR. It was the Cu ion-exchanged ZSM-5. Several different zeolite catalysts have been mentioned in the literature. As can be seen in the table, the table is divided into catalyst, conditions and NO<sub>x</sub> reduction efficiency (Müller, 2003). There are three main zeolite types and researchers have been studied for these types for 20 years (Mrad, 2015).

Table 3.4. Activity of various zeolite catalysts for HC-SCR (Mrad, 2015)

Catalyst	Reaction conditions				T <sub>max</sub> (°C)	NO reduction efficiency	
	NO (ppm)	O <sub>2</sub> (%)	Reducing agent	H <sub>2</sub> O (%)		NO conversion (%)	N <sub>2</sub> selectivity (%)
Beta-11-194	750	2.4	470 ppm C <sub>3</sub> H <sub>8</sub>		350	na	75
ZSM5-17-195	750	2.4	470 ppm C <sub>3</sub> H <sub>8</sub>		350	na	70
CuSiBEA	1000	2	1000 ppm C <sub>2</sub> H <sub>6</sub> O		380	40	78–90
CuSiBEA	1000	2	2000 ppm C <sub>3</sub> H <sub>8</sub>		380	20	90–100
Co/MFI WIE	1600	2.5	1000 ppm CH <sub>4</sub>		450	na	31
Co/MFI SUB-Cl-a	1600	2.5	1000 ppm CH <sub>4</sub>		400	na	29
Co/MFI SUB-Br-a	1600	2.5	1000 ppm CH <sub>4</sub>		425	na	34
Co/MFI WIE	2000	3	2000 ppm iso-C <sub>4</sub> H <sub>10</sub>		475	na	95
Co/MFI SUB-Cl-a	2000	3	2000 ppm iso-C <sub>4</sub> H <sub>10</sub>		400	na	99
Co/MFI SUB-Br-a	2000	3	2000 ppm iso-C <sub>4</sub> H <sub>10</sub>		425	na	99
Pd-SBA-imp	150	7	1500 ppm CH <sub>4</sub>		300	98	na
HAIBE (700)	1000	2	1000 ppm C <sub>2</sub> H <sub>6</sub> O		450	62	98
Pt-MFI-97	1000	2	1000 ppm C <sub>2</sub> H <sub>4</sub>		212	na	19.8
Co(0.91)ZSM-5	900	2	1000 ppm C <sub>3</sub> H <sub>8</sub>		450	50	na
Co(1.13)+Ca/ZSM-5	900	2	1000 ppm C <sub>3</sub> H <sub>8</sub>		500	54	na
Co(1.28)+Ba/ZSM-5	900	2	1000 ppm C <sub>3</sub> H <sub>8</sub>		500	76	na
Co(imp)-Pd(WIE)-ZSM-5	500	5	2500 ppm CH <sub>4</sub>	5	450	90	na
2% Pt/MCM-41	1000	14	3000 ppm C <sub>3</sub> H <sub>6</sub>		200	94	na
2% Pt/B-MPS	1000	14	3000 ppm C <sub>3</sub> H <sub>6</sub>		160	100	na
2% Pt/MPS	1000	1	10,000 ppm C <sub>3</sub> H <sub>6</sub>		400	100	na
Ag/Al-SBA-15 (6)	500	10	2500 ppm C <sub>2</sub> H <sub>6</sub> O		350	35	100

Ion-exchanged zeolite catalysts show great NO<sub>x</sub> conversion performance by hydrocarbons. There are some positive properties as well such as wide window temperature, and high tolerance to catalyst deactivation caused by sulfur poisoning and coke deposition. In comparison with silver oxide catalyst, the ion-exchanged zeolite displays relatively high NO<sub>x</sub> conversion and this efficiency are not significantly affected by the nature of the reducing agent. Because of the hydrothermal condition, the ion-exchanged zeolite is probably unsuitable for the realistic SCR of NO<sub>x</sub> from diesel engines. There are also Copper-aluminum oxide catalysts (Cu-Al<sub>2</sub>O<sub>3</sub>). It has been studied for the HC-SCR of NO<sub>x</sub>. In comparison

with Cu-ZSM-5, The Cu-Al<sub>2</sub>O<sub>3</sub> with 16 wt.% Cu content has higher activity at low temperature. Another positive property of Cu-Al<sub>2</sub>O<sub>3</sub> compared to Cu-ZSM-5, Cu-Al<sub>2</sub>O<sub>3</sub> exhibits greater hydrothermal stability (Sawatmongkhon, 2011).

Platinum-based catalyst is known as a splendid metal group for the reduction of NO<sub>x</sub> at low temperatures (195°C -260°C) and stability in water and sulfur (Müller, 2003). This type catalyst is unsuitable for the use in light-duty compression ignition motors where the exhaust temperature varies often between 199°C and 395°C. It is a major drawback of the Platinum-based catalyst (Sawatmongkhon, 2011).

### **3.3 Objective of The Study**

The aim of this work was to study the effects of a palladium-based (Ag-Pd-Ti) catalyst with an Adblue-Propanol blend as a reductant on the NO<sub>x</sub> conversion ratios in a diesel engine connected to a performance test that is equipped with a DOC and an HC-SCR. Throughout the experiments, many test parameters were evaluated such as the space velocity, the loading on the engine, and the amount of propanol-AdBlue mixture.



#### 4. LITERATURE REVIEW

In this chapter, former papers on the subject of diesel engines' emissions regulations, with an emphasize on NO<sub>x</sub> reduction and Hydrocarbon selective catalytic reduction have been analyzed and reviewed.

Pihl et al sought the activity condition for lean conversion of NO<sub>x</sub> over sol-gel synthesized silver alumina (Ag/Al<sub>2</sub>O<sub>3</sub>) catalysts, with and without platinum doping on condition that using ethanol (EtOH), EtOH/C<sub>3</sub>H<sub>6</sub> and EtOH/gasoline blends as reducing agents. Despite the fact that platinum doping showed progressions inactivity during the powder reactor tests, this progression was not convertible to the EtOH/gasoline conclusions for monolith samples. The major reason for the situation was various residence time for the powder and monolith tests, and likely also an effect of increased surface adsorption of aromatic compounds from the gasoline at low temperatures, which poisons the catalyst surface. The 4% Ag/Al<sub>2</sub>O<sub>3</sub> specimen displayed a greater reduction, lower onset temperature and greater formation of NH<sub>3</sub>, for all three EtOH/gasoline blends in comparison with the 2% Ag/Al<sub>2</sub>O<sub>3</sub> specimen doped with 100 ppm Pt. In other words, the 4 wt.% Ag/Al<sub>2</sub>O<sub>3</sub> catalyst showed 100% reduction in the range 340–425°C with up to 37% selectivity towards NH<sub>3</sub>. These results were also supported by DRIFTS (Diffuse reflection infrared Fourier transform spectroscopy) experiments. The high NH<sub>3</sub> formation pertains to the greater formation of isocyanates for the pristine Ag specimen in comparison with the Pt doped specimen and displays promising implications for more studies. In combination with an NH<sub>3</sub>-storage/SCR catalyst system, which could result in a decreased fuel penalty, the silver-alumina catalyst catered an influential reduction of NO<sub>x</sub> system for ethanol-powered vehicles (Phil et al., 2017).

Kumar et al examined the ammonia-SCR process with three monolith catalysts: 2.6 wt. % Cu/SAPO-34, 2.5 wt.% Cu/BEA and 3.1wt.%Cu/SSZ-13. Their ion-exchange level was 0.20, 0.56 and 0.16 respectively in the experiment.

Some reactions were sought to analyze and understand the zeolite type such as ammonia oxidation, NO oxidation, standard SCR, NO<sub>2</sub> SCR, and fast SCR. As a first step, oxidation of NO<sub>x</sub> was analyzed and the conclusion was found that Cu/BEA had higher NO oxidation than the Cu/chabazites. The studies demonstrated that the small-pore zeolites/silicoaluminophosphates with CHA structure (Cu/SAPO-34 and Cu/SSZ-13) had displayed higher SCR activity at 150°C in Standard SCR conditions and it exhibited lower N<sub>2</sub>O selection rate than Cu/BEA. Nevertheless, an ammonium nitrate sample formed over Cu/CHA catalysts was enabled to decrease of NO<sub>x</sub> conversion during fast SCR conditions at 150°C.

The formation of ammonium nitrate and its decomposition temperature made Cu/BEA more active catalytically than Cu/SAPO-34 or Cu/SSZ-13 at lower temperatures in fast SCR circumstances. Alongside, results denoted that ammonium nitrate species had more stability on the small pore zeolites than on Cu/BEA. Comparing the two Cu/CHA catalysts, Cu/SAPO-34, and Cu/SSZ-13, it was found that ammonia oxidation at high temperatures and ammonia SCR at 150°C was higher on Cu/SAPO-34. Moreover, tests showed that Cu/SAPO-34 is more easily reduced in comparison with Cu/SSZ-13. This could facilitate the redox processes and can thereby be a reason for the higher activity at 150°C for Cu/SAPO-34. Conclusions demonstrated that the formation of N<sub>2</sub>O in standard SCR was higher on Cu/BEA. Another observation attained from this experiment was the formation of N<sub>2</sub>O in standard SCR was higher on Cu/BEA. The conclusions of this experiment evidenced that the ion-exchange level had a huge effect on the activity and selectivity of the SCR operations and also the type of zeolite/silicoaluminophosphates had an effect on these properties as well (Kumar et al., 2015).

O. Hasan et al sought several parameters about the effects of three different fuels (CH<sub>4</sub>, H<sub>2</sub>, and ULSD). They primarily investigated these three fuels according to different gaseous fuel mixtures operating under real exhaust gas conditions on the

emissions of the engine, the characteristics of the combustion, and selective catalytic reduction (SCR) after treatment at low, medium, and high engine loads. The catalyst used in the study was 1% Pt/Al<sub>2</sub>O<sub>3</sub>. It was used and applied at various exhaust gas temperatures. In this experiment, the preparation method of the catalyst was the standard impregnation method using a platinum nitrate solution with the alpha-alumina ( $\alpha$ -Al<sub>2</sub>O<sub>3</sub>) phase. Pt/Al<sub>2</sub>O<sub>3</sub>-SCR reactor had been conducted at different exhaust gas temperatures. The Pt/ Al<sub>2</sub>O<sub>3</sub> SCR catalyst used in this study was designed to promote the NO<sub>x</sub> reduction at low and medium temperatures under real diesel engine exhaust conditions.

Conclusions demonstrated that the gaseous fuels (CH<sub>4</sub> and H<sub>2</sub>) have a similar change in the combustion process, and they both moderated the rate of heat release and in-cylinder. At the high engine load, there was a huge effect that appeared as an increase in the premixed combustion phase and a considerable decrease in the total combustion duration. At the high engine load, fuels with a higher amount of CH<sub>4</sub> had a tendency to reduce the formation of NO<sub>x</sub> from the point of emissions. Nevertheless, for fuel with so much H<sub>2</sub> content had a tendency to decrease emissions of PM formations. In addition to this, the combustion of tri-fuel with a 50:50 fuel mixture concluded in lower BSFC in comparison with the other ratios and, because of that reason, the best suitable engine efficiency. Under real diesel exhaust gas, hydrocarbon-SCR displayed spectacular conclusions in the reduction of NO<sub>x</sub> emissions in temperatures window of 180°C -280°C for all engine loads (Hasan et al., 2017).

Vasalos et al investigated Ag-based catalysts applying the dry impregnation technique. These Ag-based catalysts supported on unpromoted or Ce-promoted  $\gamma$ -alumina were analyzed for the selective catalytic reduction (SCR) of NO<sub>x</sub> with different reductants. The reductants studied in the experiment were C<sub>3</sub>H<sub>6</sub>, CH<sub>4</sub> and CO, C<sub>2</sub>H<sub>4</sub>, C<sub>2</sub>H<sub>6</sub>, C<sub>3</sub>H<sub>8</sub>, C<sub>4</sub>H<sub>10</sub>, 1-C<sub>4</sub>H<sub>8</sub>, and C<sub>4</sub>H<sub>6</sub>. Between C<sub>3</sub>H<sub>6</sub>, CH<sub>4</sub>, and CO, C<sub>3</sub>H<sub>6</sub> was the most important and effective reducing agent for the SCR system. Because of the oxygen-content in the reaction combination rose from 2% to 10%,

the efficiency of conversion of  $\text{NO}_x$  increased. The influence of Ag loading, the catalytic support used and the type of the reductant on  $\text{NO}_x$  reduction was examined. Whereas rising the metal loading avoided the catalytic activity, the best efficient de  $\text{NO}_x$  activity was obtained from the Moderate silver loadings (3%). Lower calcination temperature reduces the catalytic performance and activity. Because of it raised the de $\text{NO}_x$  effectiveness, great calcination temperature was selected in the experiment. Lower calcination temperature reduces the catalytic performance and activity. The reduction of  $\text{NO}_x$  was decreased as the number of C atoms raised or using more unsaturated hydrocarbons.

Higher concentrations of the optimum reductant (1-  $\text{C}_4\text{H}_8$ ) significantly enhanced the de $\text{NO}_x$  activity, attaining over 80%  $\text{NO}_x$  reduction and an interestingly broad active temperature window (300°C–550°C) (Vasalos et al., 2004).

Lanze et al investigated three main catalysts with different conditions such as different temperature ranges, various space hour velocities which are standard in diesel engines and heavy-duty trucks. Catalysts used in the study were Rh, Ag on alumina, and Pt. Catalyst preparation method was the incipient wetness technique with the following catalyst material: 2wt. %Rh/  $\text{Al}_2\text{O}_3$ , 2wt%Ag/  $\text{Al}_2\text{O}_3$ , and 2wt. %Pt/ $\text{Al}_2\text{O}_3$ . Experiments were carried out with other conditions.  $\text{C}_3\text{H}_6$  concentration was varying between 500 and 2000ppm, NO concentration was 500ppm, and Oxygen was 5% at all times. All the catalysts tested were very active in the conversion of NO and displayed various behaviors. In the end, results of experiments were obtained and these values were as follows: Silver had the highest conversion rates at 50% the least accepted conditions (high GHSV and Low  $\text{C}_3\text{H}_6$  concentration), and 80% to 100% in other conditions. At a temperature range of 350°C and 600°C, the catalyst was active, with more than 80% conversion rates at a temperature range of 400°C -550°C. The reducing agent showed a decrease in the amount at the highest temperatures because of propane combustion. Steam didn't have a significant effect on conversion rate, but  $\text{H}_2$  addition improved the

reaction and led to high conversion rates at low temperatures. Platinum and Rhodium gave lower conversions than Ag but were active at lower temperatures (200°C -400°C). Steam affected Rh severely, while C<sub>3</sub>H<sub>6</sub> concentration played a role in affecting Pt performance. For Rh, adding hydrogen showed a higher conversion rate without the need to propene, however, with the addition of C<sub>3</sub>H<sub>6</sub>, a little decrease in the performance was observed. Up to 150°C, for Pt, there was an effect like that with silver, but above 150°C, the conversion wasn't affected much (Lanze et al., 2009).

Ali Keskin et al investigated the characteristic properties of diesel engines, essential pollutant emissions, and their effects and ways to eliminate them. Pollutants are occurred because of some reasons such as unburnt fuels as a result of inadequate temperature, incomplete combustion, inadequate combustion of hydrocarbons and very high temperature in the cylinder. There are many organizations to regulate and control them such as EPA, OECD, IPCC, IEA, EEA. In particular, European Emission Standards were constructed to control and minimize emissions. Euro standards are used worldwide. CO, HC, NO<sub>x</sub>, PM are the main pollutants. Some methods were invented to eliminate the negative effects of these pollutants such as DOC, DPF, SCR, EGR, LNT. These are called aftertreatment systems. EGR is used to reduce NO<sub>x</sub> emissions whereas DOC is used to decrease CO and HC. LNT is applied to decrease NO<sub>x</sub> emissions. DPF is the main technique to reduce PM emissions. For the reduction of NO<sub>x</sub>, the most effective and important method is SCR. In particular, for heavy-duty engines, SCR is used to reduce NO<sub>x</sub> emissions. It is likely to decrease the harmful effects of the pollutant emissions both the health side and the environment side and also meet the regulation of emission standards by using after treatment techniques (Resitoglu et al.,2015).





## 5. MATERIALS AND METHODS

In this section, the ceramic materials which used in preparing the catalyst were identified and explained associated with, the chemicals used in coating the catalysts, the preparation steps of the catalyst, the specifications of the instruments used to searched the structural and chemical properties of the catalyst, the experiment setup for testing the catalyst in real conditions, the technical specifications of all the instruments related to the setup experiment, and finally, the electronic equipments and programs that were applied throughout all the conducted experiments.

### 5.1 Catalyst Preparation

Production of the catalyst was carried out using the infrastructure of the laboratories belonging to Automotive Engineering of Cukurova University. In the catalyst production, cordierite ( $2\text{Al}_2\text{O}_3\text{-5SiO}_2\text{-2MgO}$ ) and monolith's main carrier structure were used. The carrier structure was obtained commercially.

The impregnation method was used to prepare the catalyst sample. This structure has 400 cells per square inch. First of all, it was pretreated with oxalic acid so as to raise the area of the surface of the cordierite structure. After that, so as to get up the solution, a mixture including silver nitrate, titanium dioxide, and oxalic acid by weight of 5.91, 50 and 17.3 g respectively and tetra ammine palladium nitrate solution by volume 7.17 ml was dissolved via ultrasonic stirrer in 500 ml of distilled water. Then, it was dried for 1 hour in an oven at  $110^\circ\text{C}$  so as to do away with water completely. After this, calcination was applied for 4 hours at  $550^\circ\text{C}$  and then ground to obtain powder catalyst 40 g of the powder catalyst attained by this method were mixed in 500 ml of distilled water and solution containing Ag, Pd and Ti was prepared. The pretreated cordierite was immersed in the prepared solution and the pores closed during immersion were opened with a compressed air gun. Finally, the coated cordierite was dried in an oven at  $110^\circ\text{C}$  for

1 hour. After then, dipping and dehydration processes above mentioned were repeated. Finally, the carrier structure was calcined at 550°C for 3h in muffle furnace to obtain the desired catalyst. Thus, the production of catalyst containing Ag, Pd and Ti were realized. Finally, the catalyst samples for SEM/EDX, XRF, and BET analyzing were prepared in order to determine the characterization of the catalyst.

### 5.1.1 Cordierite Specifications

In the preparation of the catalyst, the cordierite ( $2\text{Al}_2\text{O}_3\text{-}5\text{SiO}_2\text{-}2\text{MgO}$ ) with a monolith honeycomb as support was applied (Figure 5.1) with the following dimensions: 103x130mm and a 400 cpsi square pores. Because of its superior hydrothermal stability, low cost and lower thermal expansion coefficient in comparison with other constructions, this structure was preferred in the experiments. Figure 5.1 and Figure 5.2 shows that monolith honeycomb and silver, copper and distilled water.



Figure 5.1. Monolith honeycomb Cordierite

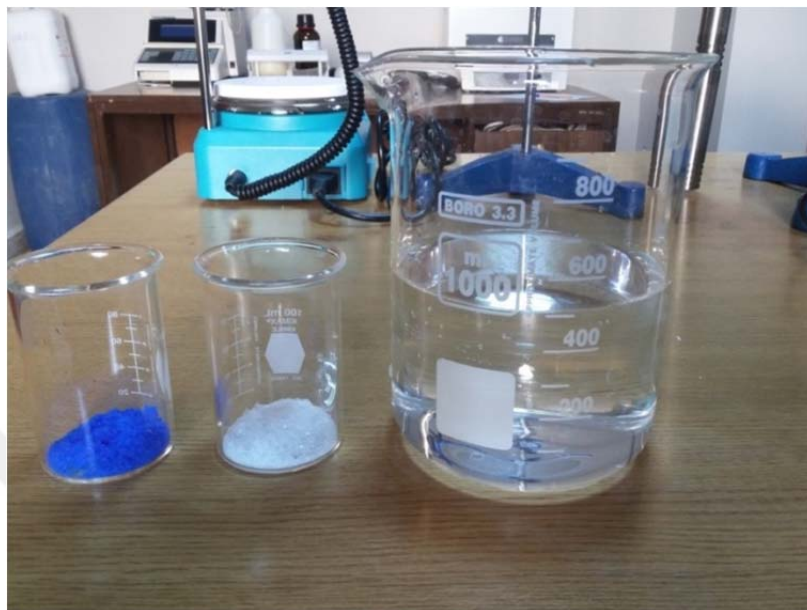


Figure 5.2. Silver, Copper and distilled water

## 5.2. Catalyst Characterization Equipment and Technical Properties:

In this section, the technical specifications of the machines used to analyze the catalysts (XRD, BET and SEM) were explained as follows:

### 5.2.1. X-ray Diffraction (XRD)

A technique was used to identify the molecular structure of crystalline material by diffracting x-rays into the sample. By obtaining interference patterns, An XRD analyzer can reflect lattice structures by modifying the incidence angle of the X-Ray beam. The X-RAY DIFFRACTOMETER (XRD) used in our thesis was the PANalytical EMPYREAN XRD (Figure 5.3) available in the Cukurova university's central research laboratories.



Figure 5.3. The PANalytical EMPYREAN XRD

Table 5.1. Technical specification of PANalytical EMPYREAN XRD

Tube	X-Ray tube,CU-Ka
Voltage range[KV]	20-50
Flow range [MA]	5-60
Goniometer diameter[mm]	480
Goniometer geometry	Perpendicular,therta-therta, and alfa-1
Smallest size of step	0.0001°( $\theta/2\theta$ ).
Scanning speed	0.0001°/minute
Angle-to-angle passing speed	500°/minute
Maximum angle	$111 < 2\theta < 168^\circ$
Detector	high-speed pixel-based
Maximum counting capacity	1x106 signal/sec
Minimum pixel space	70 micron x 70 micron
Fixed snapshot in angular field	4° (2 $\theta$ )
Mapping	2D
Model	Bragg-Brentano optic model
Collimator	Cross-slit

### 5.2.2. BET Analysis

Brunauer-Emmett-Teller (BET) Surface Area Analysis is a technique that proves to determine measures of the surface area, micro and macro pores size, and pores size distribution by physical adsorption method in solid and powder samples at low pressures and with high-resolution. The device used in the experiments was the KELVIN 1042 device which is available at the universities research labs, shown in Figure 5.4:



Figure 5.4. KELVIN 1042

Table 5.2. KELVIN 1042 technical properties

Gas volume measurement interval	0.005-20cc
Specific area that can be measured(SSA)	0.01 m <sup>2</sup> /g
Pore size[nm]	2-200
Ability	Can work with 6 sample in one cycle
Degassing Temperature	35-350°C
Analyses period	15 minutes(single point)

### 5.2.3. SEM Analysis

The scanning electron microscope (SEM) is a technique that can do analysis of solid specimens, any conducting sample that doesn't have liquid properties, metals, textiles, fibers, and plastic polymers; also, samples that are not conductive can be coated with very thin (2Å/second) conductive material and be analyzed. This process works by focusing a beam of high- energy electrons to produce different signals at the surface of the specimen. The signals obtained from electron-sample interaction provides information about the specimen like its morphology (texture), crystalline structure, the orientation of the materials available in the sample and chemical composition. In general, the data gets

collected in one area of the surface of the specimen and spatial variations are shown in a produced 2-dimensional image. In this thesis, FEI Quanta 650 Field Emission SEM (Figure 5.5) available at Cukurova University's Central Research Laboratory was used.



Figure 5.5. FEI Quanta 650 Field Emission SEM

The technical properties of the device are: Microscop's resolution; in high vacuum, in 30kV 1.2nm (SE), in 1KV 3nm (without slowing down the electron) (SE), in Low vacuum, 30kV 2nm (SE); high vacuum SE and four department BSE detector that can be summoned back; high vacuum in column SE and BSE detector; X-Ray energy distribution spectrometry; GSED (for ESEM mode) detector; STEM detector that can be called back; BSE detector that can work in low vacuum; voltage of acceleration, 100V-30kV; probe flow, 100nA; amplification: 6-1.000.000 x; camera navigation.

### 5.3 Chemical Properties of Materials Used in Catalyst Preparation

#### 5.3.1. Propanol

The central theme of this thesis was to experiment with the effects of propanol as a hydrocarbon reductant in reducing the NO<sub>x</sub> emissions in an HR-SCR system. Propanol is a clear, low-viscosity, neutral liquid with a characteristic



alcohol odor. The product is miscible with all common solvents, such as alcohols, ketones, aldehydes, ethers, glycols, and aromatic and aliphatic hydrocarbons. Propanol is also miscible in all proportions with water (Anonymous 40). Table 5.3 shows the physical properties of propanol.

Table 5.3. Physical properties of Propanol (Anonymous 41)

Synonym	Isopropanol	Beilstein Registry	635639
Molecular formula		EG/ EC Number	2006617
Molecular weight	60.10	MDL Number	MFCD00011674
CAS number	67-63-0	Vapor Pressure	33 mg Hg (20°C)
Density	0.785 g/mL at 25°C	Dielectric Constant	20.18 at 20°C
Boiling point	82°C	Dipole Moment	1.560
Melting point	-89.5°C	UV cutoff	210 nm
Flashpoint	11°C	Refractive Index	1.377 at 20°C
Viscosity(cP)	2.038 at 25°C	Vapor Density	2.1 (vs. air)
RIDADR	UN 1219 3/PG 2	Hazard Statements	H225- H319- H336
Signal Word	Danger	Precautionary Statements	P210- P261-P305+ P351+ P338

### 5.3.2. AdBlue

AdBlue® is a highly purified colorless liquid. It contains demineralized water (67.5%) and urea (32.5%). It is used with diesel engines and is also known outside of Europe as DEF, ARLA 32 or AUS 32 in some countries. The main active component of AdBlue® is ammonia. This is chemically formed by

hydrolyzing automotive urea, which is the main raw material for AdBlue. Urea is also used in the production of fertilizers and many more applications.

AdBlue is used with diesel engines using SCR technology. This technology reduces  $\text{NO}_x$  emissions. AdBlue is injected into the catalyst of the SCR system, where it triggers a chemical reaction with the ammonia. This chemical reaction converts the toxic nitrogen oxides ( $\text{NO}_x$ ) into nitrogen ( $\text{N}_2$ ) and water vapor ( $\text{H}_2\text{O}$ ). Water vapor and nitrogen are naturally occurring gasses that are harmless to the environment (Anonymous 42).

### 5.3.3. Palladium

Palladium together with rhodium, ruthenium, osmium, iridium and platinum form a group of elements referred to as the platinum group metals (PGM). Palladium is a lustrous silver-white metal. It has a face-centered cubic crystalline structure, at ordinary temperatures, it is strongly resistant to corrosion in air and to the action of acids. It is attacked by hot acids, and it dissolves in aqua regia. It forms many compounds and several complex salts. Palladium has a great ability to absorb hydrogen (up to 900 times its own volume). Palladium is used extensively in jewelry-making in certain alloys called “white gold”. It may be alloyed with platinum or substituted for it. It is used in watch bearings, springs, and balance wheels and also for mirrors in scientific instruments (Anonymous 43).

## 5.4 Technical Properties of The Devices Used in Catalyst Preparation

This section explained the properties and technical specifications of all the laboratory devices used in catalyst preparation.

**5.4.1. RADWAG AS 220. R2**

Table 5.4. Technical properties of RADWAG AS 220.R2

Maximum capacity	220 g
Minimum load	10 mg
Tare range (T)	220g
Readability (d)	0.1mg
Operating Temperature	10°- 40°C
Power Supply	12/16 VDC
Stabilization time	2s

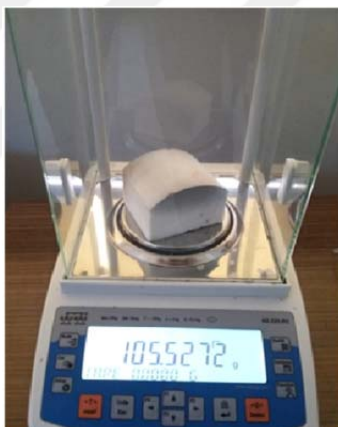


Figure 56 .RADWAG AS 220 .R2

**5.4.2. Ultrasonic Processor**

The technical properties of the Vibra-Cell V750 ultrasonic processor are given below:

Table 5.5. Vibra-Cell V750 ultrasonic processor technical properties

	Net power output	750 watts
Power supply	Frequency	20 KHz
	Dimensions (H x W x D)	235 x 190 x 340mm
	Weight	6,8 kg
Sealed converter	Part No	Piezoelectric lead zirconatetitanate cry
	Diameter	63,5 mm
	Length	183 mm
	Weight	900 g
	Cable Length	1,8 m
Standard probe	Tip Diameter	13mm with threaded end replacable tip
	Processing capability	10 ml to 250 ml
	Length	136 mm
	Weight	340 g
	Material	Titanium alloy Ti-6A-4



Figure 5.7. Vibra-Cell V750 ultrasonic processor

#### 5.4.3 Sintering Oven

The sintering process of the catalyst at 600°C for five hours was done using the Protherm Furnace Model PLF 110/6 (Figure 5.10) with the following specifications: Maximum Temperature: 1100(°C), Continuous Operating Temperature (°C): 1050; Volume (l):7.0; Inside Measurements (HxWxD) (cm): 14x20x25; Outside Measurements (HxWxD) (cm): 65x55x58; Power:1350W; Voltage:220v; Phase:1.



Figure 5.8. Protherm Furnace Model PLF 110/6

#### 5.4.4. Drying Oven

During the catalyst preparation we did a drying of the catalyst two times which was done using the Memmert BAIC oven UNB 500 with the technical specifications shown in Table 5.6.

Table 5.6. Memmert BASIC oven UNB 500 Specifications

Model	UNB 500
Chamber width A [mm]	560
Chamber height B [mm]	480
Chamber depth C [mm]	400
Oven width D [mm]	710
Oven height E [mm]	760
Oven depth F [mm]	550
Chamber volume [litre]	108
Weight [kg]	50
Power [W]	2000
Max number of trays	5
Max load per tray [kg]	30
Total load per oven [kg]	60
Ambient conditions	Ambient temperature 5°C to 40°C
Setpoint temperature range	20° C to nominal temperature

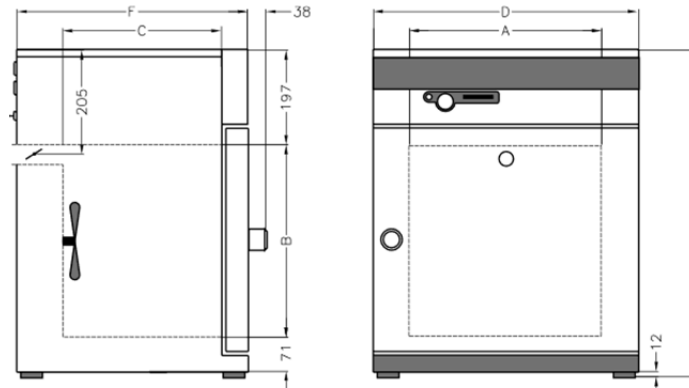


Figure 5.9. Oven Cross-sectional drawings

### 5.5. NO<sub>x</sub> Emissions Measurement System

In this section, the components and the installment processes of the NO<sub>x</sub> measurement system were explained, including the engine, the heater, the loading system, the compressor, the Matlab Simulink computer program that was employed, the loading mechanisms and the emissions control system, and its working mechanisms.

#### 5.5.1 Performance Test System Overview

To test the effects of Propanol-Adblue blends as reductants and the palladium catalyst on the efficiency of NO<sub>x</sub> reduction, an AKSA diesel engine (Figure 5.17.) available at Cukurova University Automotive Engineering Department's Laboratory was used, and to load the engine, a 10 KW electric loading system (Figure 5.20.) was used in tandem with it. The loading amount pulled by the loading system was kept constant by means of measuring the voltage and the electric current intensity. The test system generally comprises an engine, a loading system, and a specifically designed performance test system (Figure 5.12). To determine the exhaust gas flow rate aboard the system, an orifice plate was mounted onto the exhaust system. In order to adjust the exhaust gas temperatures, a heater, too, was included in the system. Temperatures were measured using k-type

thermocouples temperature sensors (Figure 5.11), installed one before DOC, and one after DOC in the exhaust system. NO<sub>x</sub> emissions reduction rates were monitored using two Continental model NO<sub>x</sub> sensors (Figure 5.11.). To extract data from these two sensors, a program was written in accordance with the CAN J1939 protocol, and using a PCAN-USB, the data extracted was recorded into the computer. To ensure the NO<sub>x</sub> reduction in the SCR system, the process of reductant spraying was composed of a multi-point (6 pores) injector and a pump that was controlled using microprocessor hardware and software. Reductant spraying was monitored electronically using a Matlab Simulink program on the computer that took measures of the spraying flow rates, an Arduino MEGA 2560 microprocessor (figure 5.14), and I/O cards. While the injector PWM was being operated under control, the pump was also, at the same time, being operated with an On-Off control mode. The space velocity of the gas flow; space velocity [SV (h<sup>-1</sup>)] is the ratio of exhaust gas volumetric flow [V<sub>f</sub> (m<sup>3</sup>/h)] to catalyst volume [V<sub>c</sub> (m<sup>3</sup>)] (Reşitoglu, 2015) was measured using a manometer with an orifice plate.

The experiments were done employing several variations like two variations of space velocity values (30000h<sup>-1</sup>), one engine load (1 KW) and finally reductant blend ratio variations (90% propanol and 10% Adblue). To determine the efficiency and performance of using the prepared catalyst with the hydrocarbon reductant in reducing NO<sub>x</sub> emissions, especially at low temperatures, NO<sub>x</sub> emissions rates were measured in the temperature window of 170°C -300°C. The experiment was conducted more than one time to ascertain the data obtained.



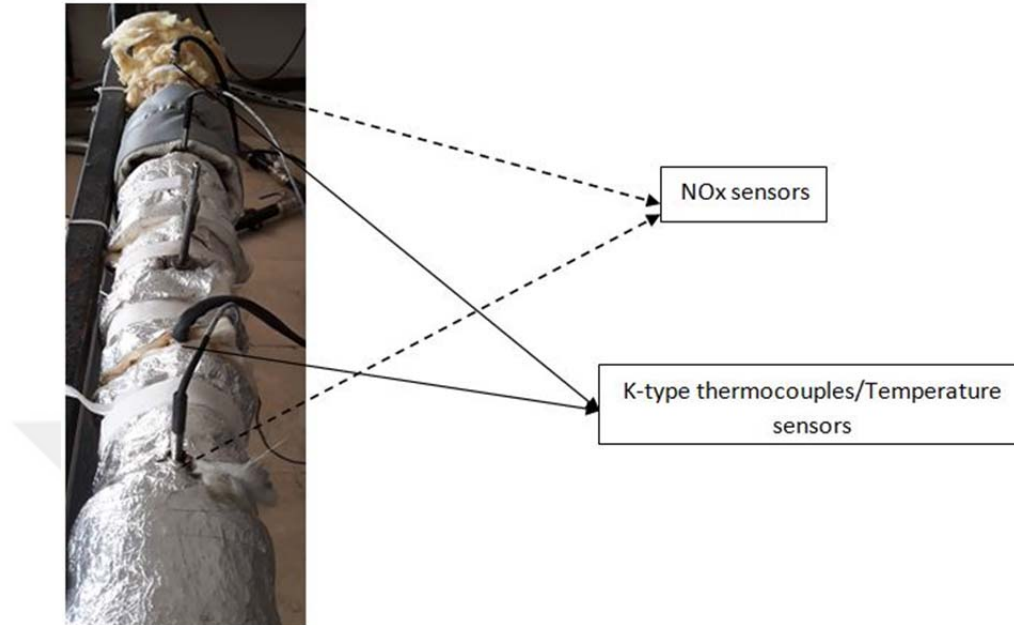


Figure 5.10. Exhaust pipe showing the NO<sub>x</sub> sensors and the K-type thermocouple

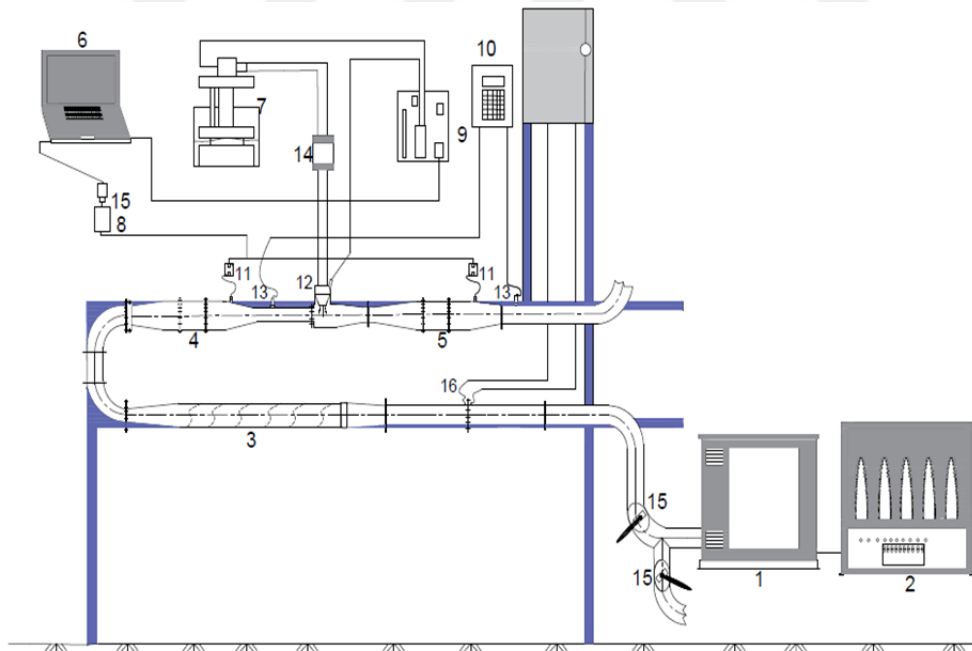


Figure 5.11. Layout of the experiment

The layout of the experiment materials are listed below:

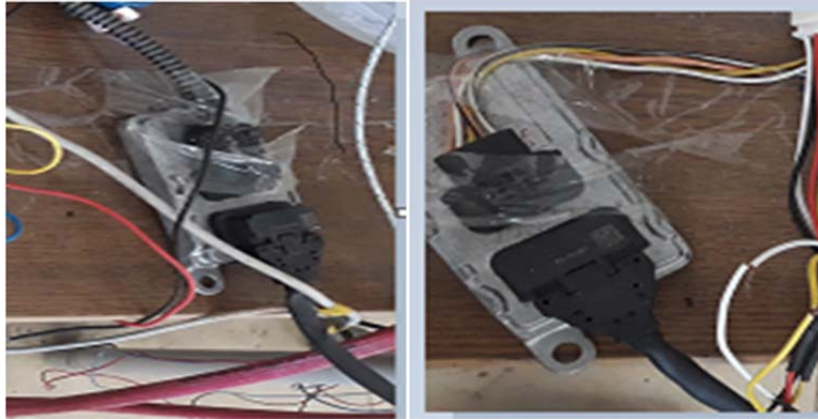
1-Engine, 2-Electric loading system, 3-exhaust gas heating department, 4-DOC (Diesel oxidation catalyst), 5-SCR (selective catalytic reduction), 6-SCR control unit, 7-reducing agent (Propanol&Adblue), 8-24V power source, 9-injector spraying control unit, 10-Digital temperature measurement device, 11- NO<sub>x</sub> sensor, 12-injector, 13-temperature sensor, 14-reductant liquid filter, 15-manual valve, 16-Orifice Plate.

### **5.5.2 Technical Properties of Test System Components**

In this section, the technical properties of the appliances used in test performance were explained.

#### **5.5.2.1 NO<sub>x</sub> Sensors**

Throughout the experiment, NO<sub>x</sub> emissions rate were the most important parameters to keep up with and measure in the experiments. The NO<sub>x</sub> gas emissions changed according to the engine working conditions. In the experiment setup, two NO<sub>x</sub> sensors were placed one before the SCR catalyst and one after the SCR catalyst; the first sensor was used to measure the NO<sub>x</sub> emissions before spraying the propanol-AdBlue reductant, and the second sensor was placed to measure the NO<sub>x</sub> emissions after the reductant spray, due to the fact that a comparison can be realized. In Figure 5.12, a Continental UniNO<sub>x</sub> sensor is shown, the sensor communication was done according to CAN J1939 protocol.

Figure 5.12 .Continental NO<sub>x</sub> sensors

#### 5.5.2.2. Arduino MEGA 2560

Arduino MEGA 2560 was uploaded with a program (code) and used together with Matlab Simulink on the computer to control the pump flow and speed of the reductant spraying. The technical specifications of which are:

Table 5.7 .Arduino MEGA 2560 Specifications

Microcontroller	Atmega2560
Operating Voltage	5V
Input Voltage (recommended)	7-12 V
Input Voltage (limits)	6-20 V
Digital I/O pins	54 (of which 14 provide PWM output)
Analog Input pins	16
DC current per I/O Pin	40Ma
DC current for 3.3V Pin	50Ma
Flash memory	256KB of which 8KB used by bootloader

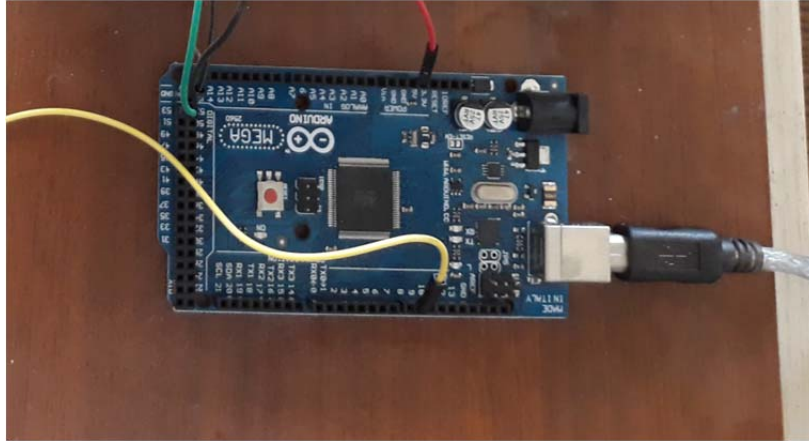


Figure 5.13 . Arduino MEGA 2560

### 5.5.2.3 Pump

A gasoline pump available at the Cukurova University Lab was used in the experiments to reductants with a multi-points (six pores) reductant injector. The pump is connected to an Arduino MEGA 2560 which in turn is connected to a Matlab program to monitor the spraying flow.

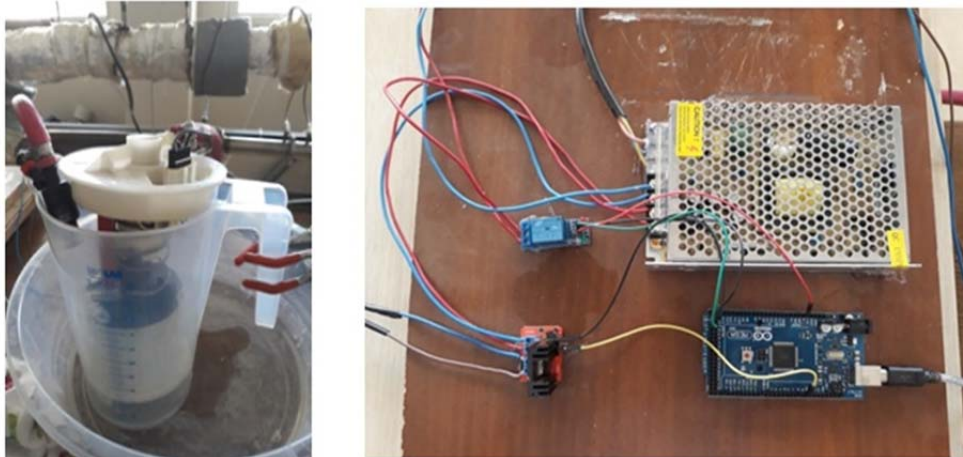


Figure 5.14 .A pump connected to an Arduino

#### 5.5.2.4 Generator

To test the NO<sub>x</sub> reduction system and conduct our lab experiments an AKSA A2CRX08 2-cylinder V-type diesel engine was used. The technical specifications of the motor are shown in Table 5.8.

Table 5.8. AKSA A2CRX08 technical properties

Model	APD 12EM
Prime frequency (Hz)	50
prime power (KVA)	8.8
Standby power (KVA)	9.6
Nominal voltage (V)	230
Nominal flow (A)	38
R.P.M (r/min)	3000
PHASE	1p
Power factor (cos <sup>φ</sup> )	1
Warning mode	Brushless capacitor
Oil capacity	2.3
Water capacity	6.4
Fuel tank capacity	15
Fuel consumption (L/h)	4
Battery voltage	12V DC
Dimensions (mm)	L=1158 W=775 H=1017
Cylinder volume (cm <sup>3</sup> )	794
Stroke (mm)	79
Cooling mode	Water
Compression ratio	23/1



Figure 5.15 .AKSA generator

#### 5.5.2.5 Orifice Plate and Manometer

A manometer and an orifice plate were installed in the system and connected to the exhaust pipe to calculate the hourly space velocity using Bernoulli's equation. The manometer is filled with water and the desired space velocity ( $30000\text{h}^{-1}$ ) corresponds to a certain water level difference in the tube measured by a millimeter.



Figure 5.16. Manometer with an orifice plate

#### 5.5.2.6. Emission Measuring Equipment

To measure exhaust gas emissions from the engine, an MRU DELTA 1600-V was used with the following technical properties:

Measuring ranges and other data;

- CO: 0-10 %
- CO<sub>2</sub>: 0-20 %
- O<sub>2</sub>: 0- 22 %
- NO: 0-4.000 ppm
- NO<sub>2</sub>: 0-1.000 ppm
- C<sub>x</sub> H<sub>y</sub>: 0-20.000 ppm
- Display: 10 - lines, backlit graphical display
- Weight: appr. 10 kg
- Dimensions: 530x490x310 mm



Figure 5.17. MRU DELTA 1600-V

#### 5.5.2.7. Thermocouple Thermometer

To measure the temperatures during the experiments a KJTRSE thermocouple thermometer logger 9682 was used with following specifications:

- K temperature range and Accuracy: 200-1370°C; (0.3% rdg +0.7°C)
- J temperature range and Accuracy: 200-760°C; (0.3% rdg +0.7°C)
- T temperature range and Accuracy: 200-390°C; (0.3% rdg +0.7°C)
- R temperature range and Accuracy: 0-1760°C; (0.3% rdg +0.7°C)
- S temperature range and Accuracy: 0-1760°C; (0.3% rdg +0.7°C)
- E temperature range and Accuracy: 200-736°C;(0.3% rdg +0.7°C)
- Resolution: 0.1°C
- LCD size(mm,HxW): 26(H)x 45(W) mm
- Operating temp: 0-50°C
- Operating RH%: Humidity<80%
- Storage temp: 20-50°C
- Storage RH%: Humidity<90%
- Dimension (mm,LxWxT): 170x70x40(H) mm
- Weight: 210g





Figure 5.18. KJTRSE thermocouple thermometer logger 9682

#### 5.5.2.8. Electric Loading System

The motor was loaded using a 10KW loading system available at the automotive laboratory (Figure 5.19). The  $\text{NO}_x$  emissions rates witnessed a significant change among different loads (1KW, 2KW, 3KW and 4KW).



Figure 5.19 . Electric loading system

## 6. RESULTS AND DISCUSSION

In this chapter, the experimental and laboratory results of catalyst characterizations (SEM, BET and XRD) and performance test results of an experiment conducted in the laboratory so as to study the effect of Propanol-AdBlue blends and Ag based catalyst on NO<sub>x</sub> conversion rates were presented and discussed with an overall conclusion and recommendations for future work.

### 6.1 Catalyst Characterization Results

#### 6.1.1. SEM Analysis Results

The photographs seen in Figure 6.1 shows the SEM images of the cordierite before and after coating with Pd taken in different scales (5000x and 10000x) and resolutions (5micrometer, 10micrometer). The mapping of the elements on the cordierite is shown in different colors in Figure 6.3. SEM images of the cordierites represent generally the cross-section of nanowires arrangements on the monolith cordierite and show how the nanoscale organization of the cordierite looks like. We can see with the high resolution (10000x) SEM image (Figure 6.1) how the cordierite is composed of a porous structure.

The first figure (Figure 6.1) shows the two SEM images results of the cordierite at 5000x resolution and 10 micrometers (upper image), 1000x resolution and scale of 5 micrometers (lower image). The second figure (Figure 6.2) displays photographs of two SEM images of the catalyst, the upper image with a resolution of 5000x and a scale of 5 micrometers, the lower image with a resolution of 10000x and a scale of 4 micrometers.

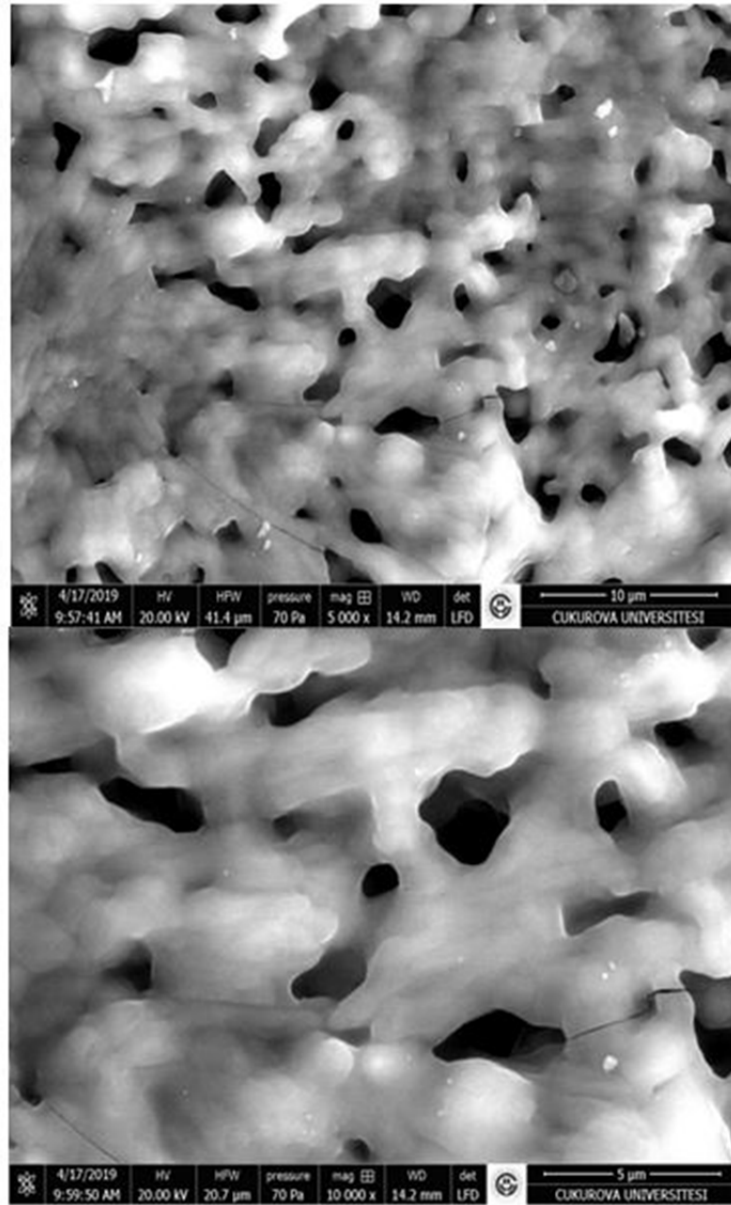


Figure 6.1. SEM images of the cordierite

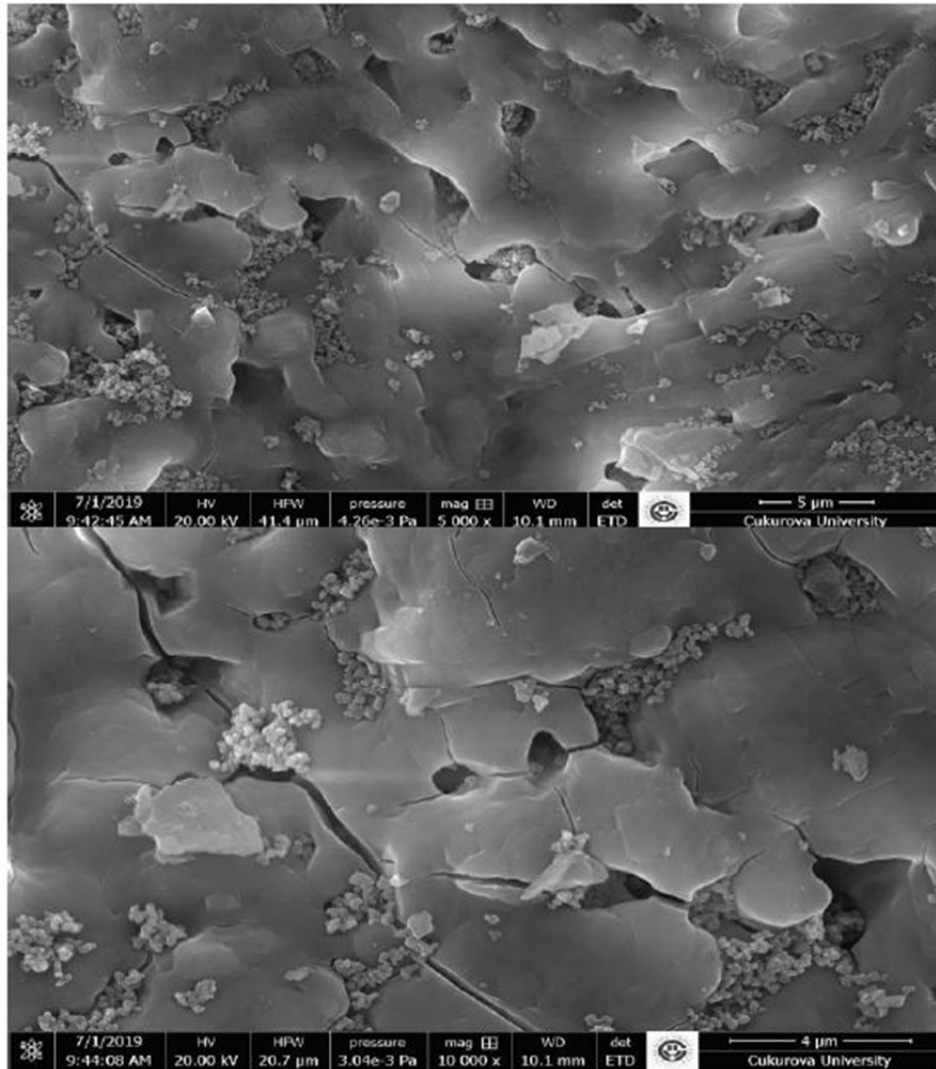


Figure 6.2. SEM images of the prepared catalyst

The first figure demonstrates that the cordierite has an irregular surface with a large number of uneven pores. When the SEM images are examined, silver, palladium, and titanium nanoparticles are observed to cling on the surface of the cordierite structure. The morphological structure of the catalyst after the coating has not changed, but it is determined that there are aggregation, spherical and oval

shapes on its surface. The shape and size of the metal nanoparticles are different and irregular. Small and well-dispersed particles make the catalyst more efficient. The SEM images indicate that the coating process has been performed successfully. The catalyst to be used in the SCR system has the desired property.

In the mapping analysis process of Figure 6.3, the observation of the coating elements (Pd and Ti) that are supposed to exhibit a catalytic activity on the coating surface of the catalyst were distributed evenly or homogeneously on the surface. The green spots in the images correspond to the palladium particles (Pd) and the pink spots to the titanium (Ti). In conclusion, the investigation of the analysis done by the SEM device and the results obtained by the microscopic and mapping proved following in check:

-A catalyst with a porous structure,

-The coating is done homogeneously across the surface,

-Elements whole penetration of the catalyst surface.

-

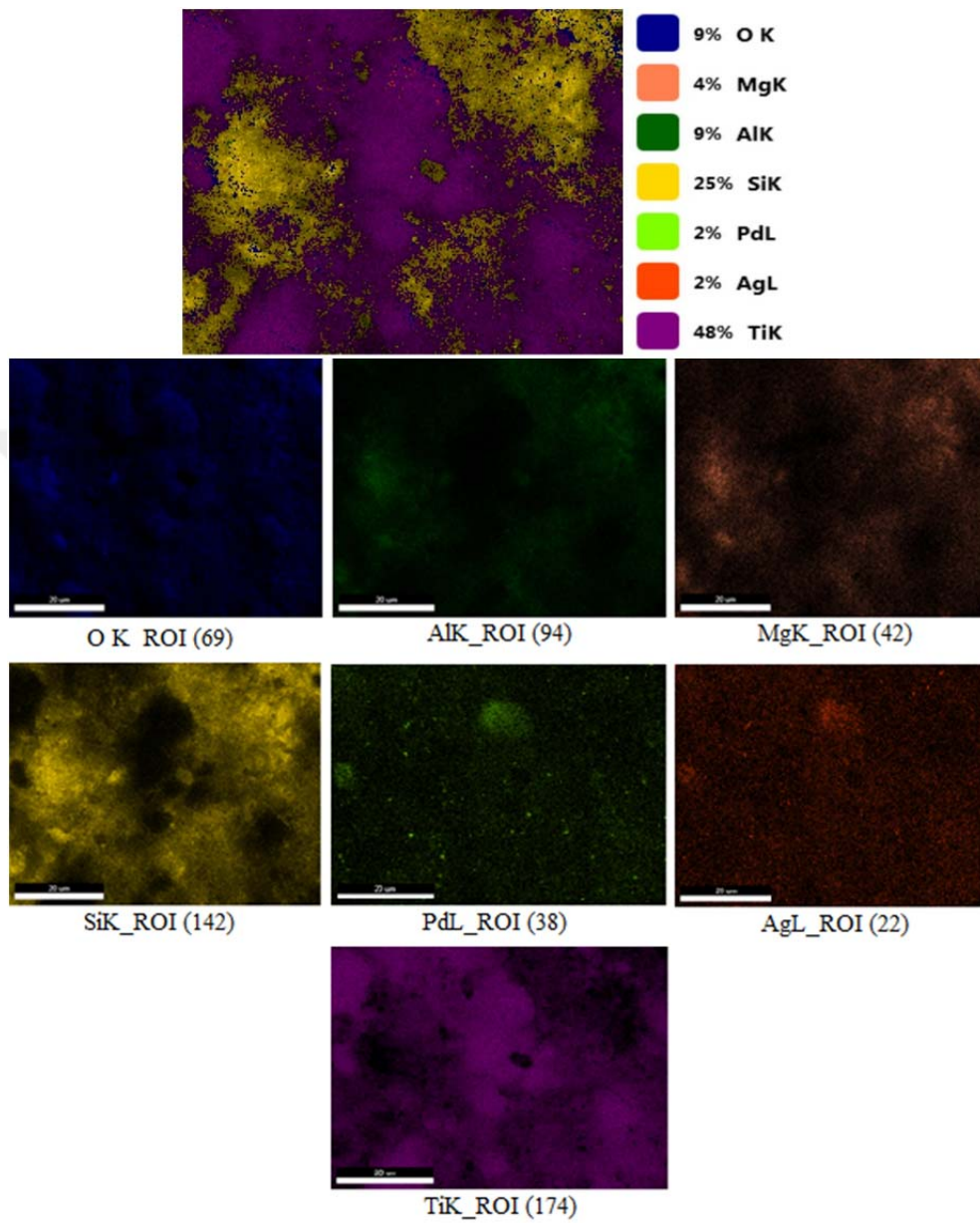


Figure 6.3. Mapping images of the catalyst

### 6.1.2. XRD Analysis Results

The Cordierite ( $2\text{Al}_2\text{O}_3\cdot 5\text{SiO}_2\cdot 2\text{MgO}$ ) before and after impregnation XRD's results are shown in Figure 6.4 and Figure 6.5 respectively.

In the pattern, the cordierite peaks are in the orthorhombic phase structure. Intensity peaks are determined at  $10.4^\circ$ ,  $10.5^\circ$ ,  $18.1^\circ$ ,  $21.8^\circ$ ,  $26.4^\circ$ ,  $28.6^\circ$ , and  $29.5^\circ$ .

The XRD peaks showed the cordierite ( $\text{H}_{0.9}\text{Al}_4\text{Mg}_2\text{O}_{18.45}\text{Si}_5$ ) in the orthorhombic phase structure, the palladinite (OPd) in the tetragonal phase structure. Intensity peaks belonging OPd are determined at  $33.7^\circ$ ,  $34.1^\circ$ ,  $55.1^\circ$ ,  $60.5^\circ$ ,  $72.1^\circ$ .

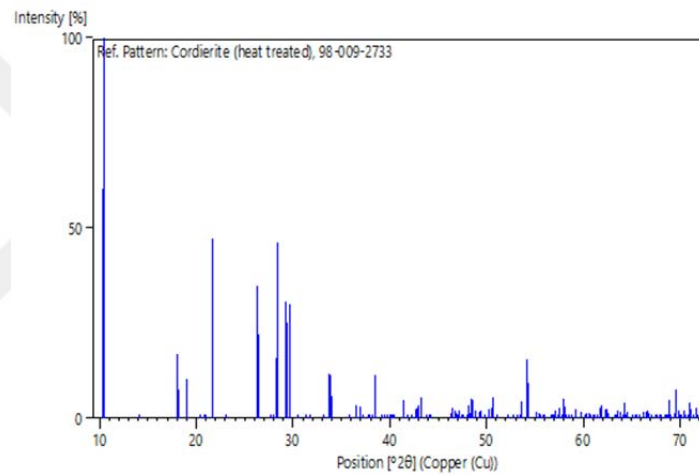


Figure 6.4. XRD results of the cordierite

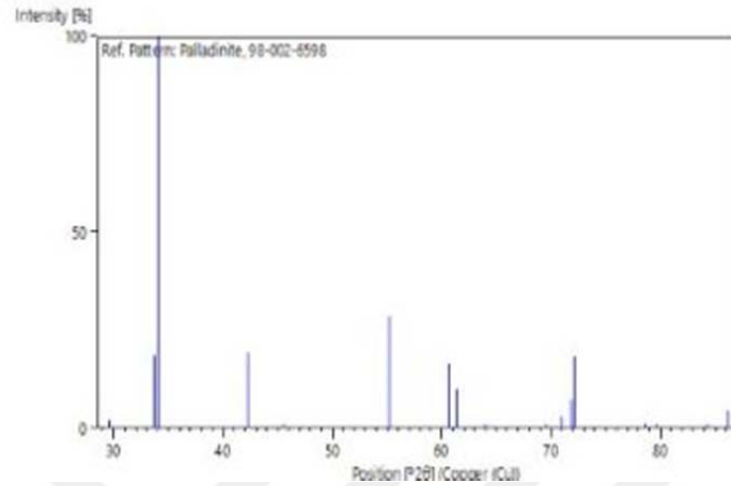


Figure 6.5. XRD results of the catalyst

### 6.1.3. BET Analysis

The BET data for the cordierite structure and synthesized catalyst are given in Table 6.1.

Table 6.1. BET analysis of cordierite and Ag-Pd-Ti catalyst

Sample	BET Surface Area, sq.m/g	Langmuir Surface Area, sq.m/g	Micropore Volume, mm <sup>3</sup> /g
Cordierite	104,715	127,847	46,864
Ag-Pd-Ti Cordierite	19,07	25,228	0,301

The BET specific surface areas of synthesized catalyst and cordierite are about 19.07 sq.m/g and 104,715 sq.m/g, respectively. Compared with the cordierite main structure, a decrease of about 82% in the BET surface area of the synthesized catalyst was observed. Furthermore, the Langmuir surface areas based on monolayer adsorption of synthesized catalyst and cordierite are found to be 25.228



sq.m/g and 127,847 sq.m/g, respectively. The micropore volume of the cordierite structure was measured as 46,864 cub.mm/g, whereas this value was 0.301 cub.mm/g for the synthesized catalyst.

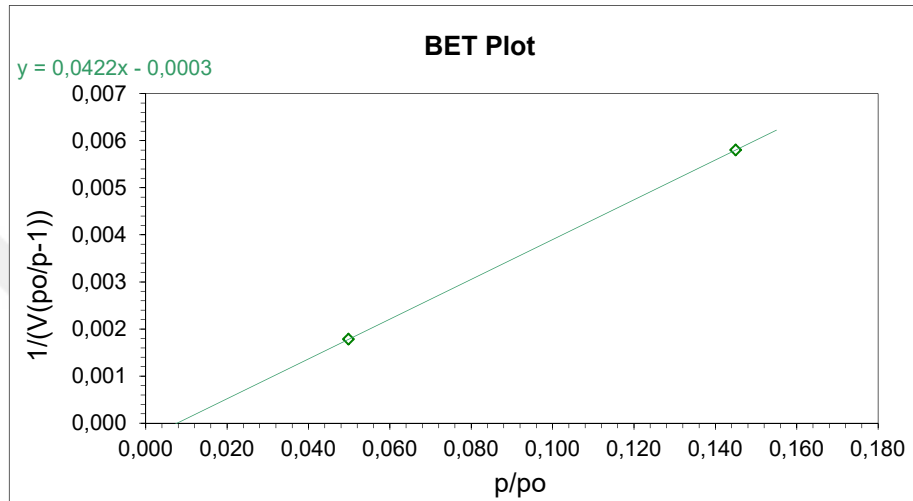


Figure 6.6. Cordierite BET plot

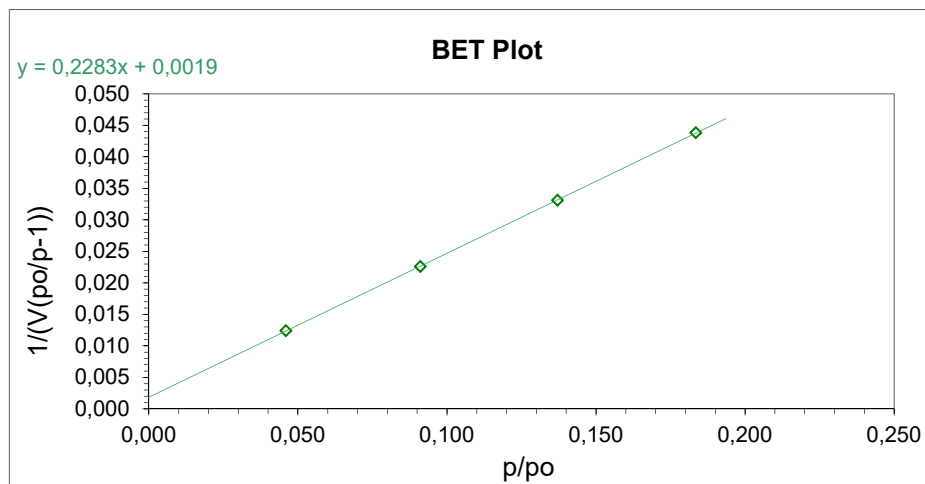


Figure 6.7. Catalyst BET plo

### 6.2. NO<sub>x</sub> Conversion Rates

In this section, the results of the test engine experiments with a catalyst and Propanol-AdBlue blends as reductant and its effects on the NO<sub>x</sub> conversion rates were discussed according to temperature, loading, spraying ratios, and space velocity. In the experiments, the NO<sub>x</sub> conversion rates were measured in four different loads (1KW, 2KW, 3KW, and 4KW), 1 space velocity (30000h<sup>-1</sup>), the temperature range of (170°C-300°C) and with different propanol to AdBlue ratio (100:0, 95:5 90:10).

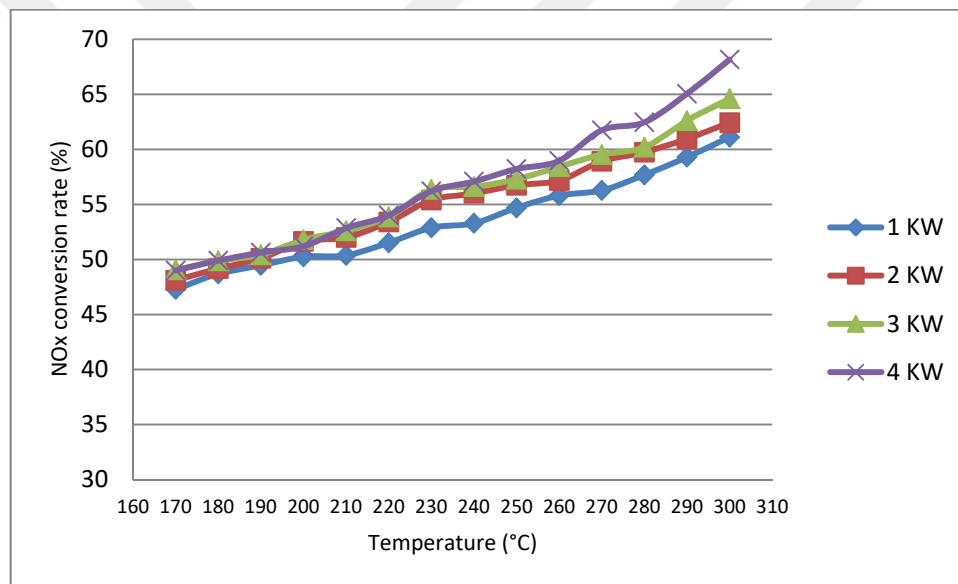


Figure 6.8. NO<sub>x</sub> conversion rate at 30000h<sup>-1</sup>/1-4 KW/ Propanol %100

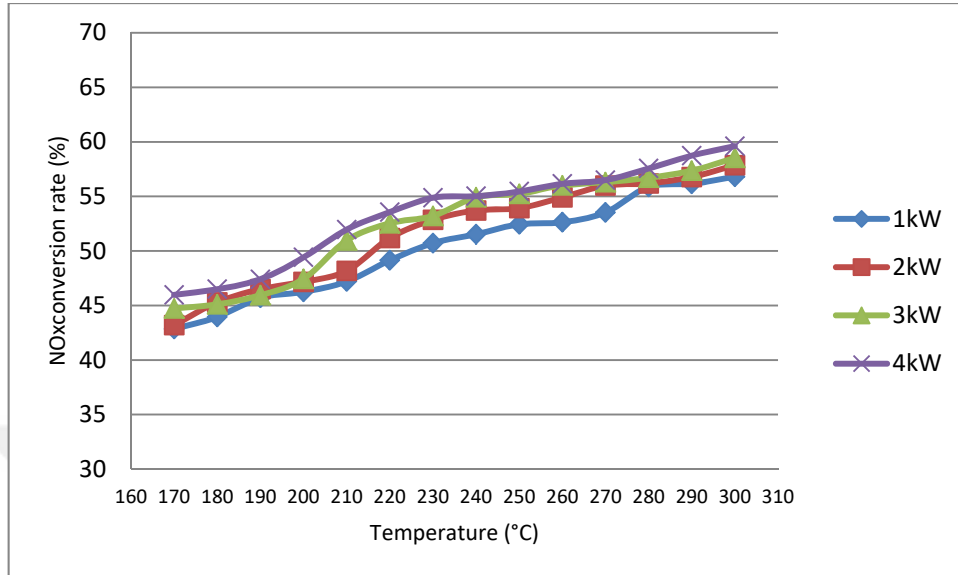


Figure 6.9. NO<sub>x</sub> conversion rate at 30000h<sup>-1</sup>/1-4 KW/ Propanol %95 - Adblue%5

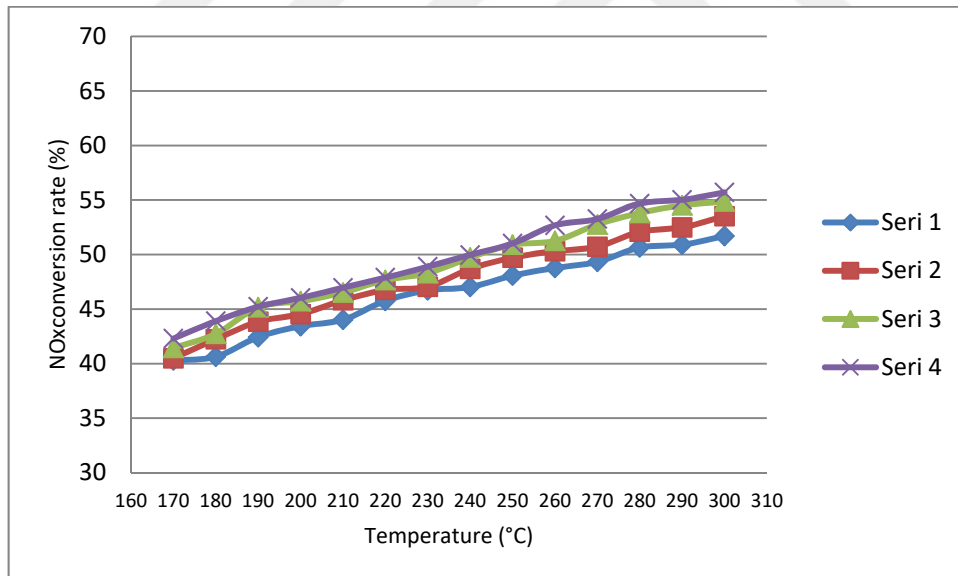


Figure 6.10. NO<sub>x</sub> conversion rate at 30000h<sup>-1</sup>/1-4 KW/ Propanol %90 - Adblue%10

### 6.2.1. Temperature Effect

According to the Figure 6.8, Figure 6.9 and Figure 6.10, the NO<sub>x</sub> conversion rate increased when the temperature increased. In Figure 6.9, NO<sub>x</sub> conversion rates showed an increase from 47,28% peaking 61,11% with uniform directions along with the trends with a temperature range between 170°C -300°C at 1 KW. Figure 6.10 also showed similar trends of NO<sub>x</sub> conversion rates starting at 42,85% and peaking at 56,81% with a temperature range between 170°C -300°C at 1 KW. Figure 6.8, Figure 6.9 and Figure 6.10 showed increasing in NO<sub>x</sub> conversion rates along with temperature increased, with peak conversion rates of 68%, 59% and 55%, respectively at T=300°C. Maximum conversion ratios were acquired at T=300°C in all engine loads. All three essential experiments demonstrated the same behaviour when the proportions of the reducing agent changed. The effect of the exhaust gas temperature on the catalyst performance was high. The scale up in exhaust gas temperature had an effect of rising the catalyst efficiency. Consequentially, the temperature had a proportional effect on the NO<sub>x</sub> conversion rates; whenever the temperature increased, the increase of the NO<sub>x</sub> conversion rates followed.

### 6.2.2. Engine Loading Effects

According to the Figure 6.8, Figure 6.9 and Figure 6.10, the NO<sub>x</sub> conversion rate increased when the engine load increased. In all the main figures, it was shown that, at the same temperature, when the engine load increased, NO<sub>x</sub> conversion increased. The average NO<sub>x</sub> conversion ratio of all reductants at 4 KW engine loads when T=300°C was found 8.17 % higher than the average NO<sub>x</sub> conversion ratio of all reductants at 1 KW engine loads. The best results were obtained in all figures when the engine load was 4 KW. The increase in engine load heightens the mixture in the cylinder, which results in an increase in both the HC content of the exhaust gas content and exhaust gas temperature to improve the

conversion efficiency. The overall conclusion was that loading at 4KW (300°C-100% Propanol) provided the best NO<sub>x</sub> conversion results (68,16%).

### 6.2.3. Blend Ratio Effects

According to the Figure 6.8, Figure 6.9 and Figure 6.10, the NO<sub>x</sub> conversion rate decreased when the proportion of AdBlue contents increased. In Figure 6.8, at 200°C and 1 KW, NO<sub>x</sub> conversion rate was 50,24% (100% propanol) but in Figure 6.9 (95% propanol- 5% AdBlue) and in Figure 6.10 (90% propanol- 10% AdBlue), at the same engine load and temperature, results were obtained 46,25% and 43,44%, respectively. In all figures, propanol showed better NO<sub>x</sub> conversion performance comparison to AdBlue. It was inferred from the results that AdBlue had negative effects on the performance of the catalyst and thus lower conversion rates were obtained.

### 6.2.4. Maximum Conversion Rate Recorded

The maximum NO<sub>x</sub> conversion rates were 68,16% rates at SV=30000h<sup>-1</sup>, motor loading=4KW, and 100% Propanol blending ratio.

## 6.3. Conclusion and Recommendations

### 6.3.1. Conclusion

The work done in this thesis on the after engine exhaust control system involved a palladium catalyst preparation using the impregnation method, to determine the catalyst characteristics, SEM, BET, and XRD analysis were conducted, in the SEM analysis, it was observed that the prepared catalyst had a porous structure, that the coatings of the catalyst spread homogeneously over its surface, and that the coating materials penetrated its surface. In The BET analysis, the surface area of the catalyst was determined, and the XRD analysis proved SEM analysis results with the peaks that are thought to represent the coating materials copper and silver, and thus showed the crystal and microstructure of the catalyst.

To test the prepared catalyst (Ag-Pd-Ti) in real-time conditions, specific test performance was installed in the laboratory of the automotive engineering department at Cukurova University. The exhaust system consisted of sensors, heater, pump, electronic control system, computer programs which monitored the NO<sub>x</sub> flow rates and hydrocarbon spray rate, DOC, and SCR system with all the accompanying components for monitoring and control. This emission exhaust system was installed after the diesel engine and the loading system. The Pd based catalyst was tested with Propanol-AdBlue blend as a reductant in various conditions of engine loading (1KW, 2KW, 3KW, 4KW), Blend ratios, and one space velocity (30000h<sup>-1</sup>). The total of the experiments conducted was three experiments.

The results demonstrated that the NO<sub>x</sub> conversion rate increased when the temperature increased. Increase in exhaust gas temperature resulted in enhancement in catalytic activity of the catalyst. This can be attributed to increase length of the hydrocarbon chain of the reducing agent molecules. On the other hand, it was shown that the increase in engine load caused an increase in NO<sub>x</sub> conversion efficiency, the best conversion rates were obtained at 4 KW engine load. It was also inferred from the results that AdBlue had negative effects on the performance of the catalyst and thus lower conversion rates were obtained. Higher conversion rates were obtained when 100% propanol was used as a reducing agent. The maximum NO<sub>x</sub> conversion rate was recorded throughout the experiment was 68,16% rates at SV=30000h<sup>-1</sup>, motor loading=4KW, and 100% Propanol blend ratio.

### 6.3.2. Recommendations

In Turkey, scientific research and development in the field of after engine emissions are limited. This is why any addition to the literature would serve as a push toward getting better solutions to eliminate diesel engines exhaust NO<sub>x</sub>

emissions. The results obtained in this thesis might serve as a reference to future research in after-engine emissions regulations.



## REFERENCES

- Abu-Jrai A.M., Al-Muhtaseb A, H., Ahmad O. Hasan.,(2017). Combustion, performance, and selective catalytic reduction of NO<sub>x</sub> for a diesel engine operated with combined tri fuel (H<sub>2</sub>, CH<sub>4</sub>, and conventional diesel). *Energy*,119,901-910.
- Andreas Å., Anders W., Jens A., Jakob K., (2016). Parameter estimation and analysis of an automotive heavy-duty SCR catalyst model. *Chemical Engineering Science*, vol.161, pp 167-177.
- Asima S., Motoi S., Kunio S., Hideaki H, (2013). Physical mixture of Ag/Al<sub>2</sub>O<sub>3</sub> and Zn/ZSM-5 as an active catalyst component for selective catalytic reduction of NO<sub>x</sub> with n-C<sub>10</sub>H<sub>22</sub>. *Applied Catalysis A: General*, 466 179– 184.
- Fredrik G, Josh A. P., Todd J. T., Magnus S,Hanna H., (2017). Lean NO<sub>x</sub> reduction over Ag/alumina catalysts via ethanol-SCR using ethanol/gasoline blends. *Applied Catalysis B: Environmental*, 202 , 42–50.
- Gill S.S., 2012. Controlling Diesel NO<sub>x</sub> & PM Emissions using fuel Components and enhanced after treatment techniques. Doctor of philosophy, School of Mechanical Engineering, The University of Birmingham.
- Guangyan X., Jinzhu M., Guangzhi H., Yunbo Y., Hong H., (2017). An alumina-supported silver catalyst with high water tolerance for H<sub>2</sub> assisted C<sub>3</sub>H<sub>6</sub>-SCR of NO<sub>x</sub>. *Applied Catalysis B: Environmental*, 207, 60–71.
- Hendry Sakke Tira., 2013. Impact Of Alternative Fuels And Hydrogen – Enriched Gaseous Fuel On Combustion And Emissions In Diesel Engines. Doctor of Philosophy, Birmingham University
- Huddleston, N., 2012, “Climate Change: Evidence, Impacts and Choices,” PDF Booklet, Washington, DC: The National Academies Press.



- Hyuk J.,(2004).Selective catalytic reduction (SCR) of nitric oxide(NO) with ammonia over vanadia-based and pillared interlayer clay-based catalysts. Master of Science, Texas A&M University.
- Iliopoulou E.F., Evdou, A.P., Lemonidou, A.A., Vasalos, I.A., (2004). Ag/alumina catalysts for the selective catalytic reduction of NO<sub>x</sub> using various reductant, *Applied Catalysis A: General*, 274, 179–189.
- International Energy Agency, 2012, “CO<sub>2</sub> Emissions from Fuel Combustion 2012,” Paris, International Energy Agency.
- King R.T., 2007. Design of a Selective Catalytic Reduction System to Reduce NO<sub>x</sub> Emissions of the 2003 West Virginia University Future Truck. Master of Science, Department of Mechanical and Aerospace Engineering, Morgantown, WV.
- Lanza R, E, E., Pettersson I.J.(2009)"NO<sub>x</sub> selective catalytic reduction over supported metallic catalysts. *Catalysis Today*, 147S, S279-S284.
- Leistner K, M, O., Wijayantia K., Kumarb A.,Kamasamudramb K., Currierb N,W., Yezeretsb A., Olsson L.,(2015). Comparison of Cu/BEA, Cu/SSZ-13 and Cu/SAPO-34 for ammonia-SCR reactions. *Catalysis Today*,258, 49-55.
- Levitus, S., Antonov, J. I., Boyer, T. P., Baranova, O. K., Garcia, H. E., Locarnini, R. A., . . . Yarosh, E. S., 2012, “World Ocean Heat Content and Thermohaline Sea Level Change (0-2000 m), 1955-2010,” *Geophysical Research Letters*, 39(10).
- Meysignac, B. and Cazenave, A., 2012, “Sea level: a Review of Present-Day and Recent-Past Changes and Variability,” *Journal of Geodynamics*, 58, pp. 96-109.
- Müller, W., Ölschlegel, H., Schäfer, A., Hakim, N. et al., "Selective Catalytic Reduction - Europe's NO<sub>x</sub> Reduction Technology," SAE Technical Paper 2003-01-2304, 2003.

- Radtke F., 1996. Selective Catalytic Reduction of NO<sub>x</sub> by Olefins". of Doctor of Technical Sciences, Swiss federal institute of technology zurich.
- Raya M, B, C., Aissa A, B., Renaud C, B., Dominique C, B., Stéphane S., (2015). Catalysts for NO<sub>x</sub> selective catalytic reduction by hydrocarbons (HC-SCR). *Applied Catalysis A: General*, 504, 542–548.
- Resitoglu I.A., Keskin A., (2017).; Hydrogen applications in selective catalytic reduction of NO<sub>x</sub> emissions from diesel engines. *International Journal of Hydrogen Energy*, vol. 42, pp. 23389-23484.
- Resitoglu I.A., Altinisik K., Keskin A., (2015). The pollutant emissions from diesel-engine vehicles and exhaust aftertreatment systems. *Clean Technologies and Environmental Policy*, vol.17, pp.15–27.
- Sawatmongkhon B., (2011). Modelling of catalytic aftertreatment of NO<sub>x</sub> emissions using hydrocarbon as a reductant,. School of Mechanical Engineering ,The University of Birmingham.
- Sitshebo S, W,T., 2010. HC-SCR of NO<sub>x</sub> emissions over Ag-Al<sub>2</sub>O<sub>3</sub> catalysts using diesel fuels as a reductant. Doctor of Philosophy, School of Mechanical Engineering,The University of Birmingham.
- Wang, J., Peng, Z., Chen, Y., Bao, W., Chang, L., Feng, G., 2015. In-situ hydrothermal synthesis of Cu-SSZ-13/cordierite for the catalytic removal of NO<sub>x</sub> from diesel vehicles by NH<sub>3</sub>, *Chemical Engineering Journal*, 263, 9-19.
- Xia, M., Viera-Hutchins, L., Garcia-Lloret, M., Rivas, M. N., Wise, P., McGhee, S. A., . . . Chatila, T. A., 2015, “Vehicular Exhaust Particles Promote Allergic Airway Inflammation Through an Aryl Hydrocarbon ReceptorNotch Signaling Cascade,” *Journal of Allergy and Clinical Immunology*, 136(2), pp. 441-453.
- Anonymous 1: <https://climate.nasa.gov/resources/global-warming/>
- Anonymous 2: <https://socratic.org/questions/how-is-the-greenhouse-effect-related-to-global-warming>

- Anonymous 3: <https://www.gsi.ie/en-ie/geoscience-topics/climate-change/Pages/Causes-and-the-greenhouse-effect.aspx>
- Anonymous 4: <https://timeforchange.org/CO2-cause-of-global-warming>
- Anonymous 5: <https://www.epa.gov/climate-indicators/greenhouse-gases>
- Anonymous 6: <https://www.eea.europa.eu/airs/2018/resource-efficiency-and-low-carbon-economy/transport-ghg-emissions>
- Anonymous 7: <https://www.who.int/sustainable-development/transport/health-risks/air-pollution/en/>
- Anonymous 8: [http://www.eng.auburn.edu/~pjones/MECH.5830.6830.6836/Internal\\_Combustion\\_Engines\\_Fundamentals\\_by\\_J.B.Heywood.pdf](http://www.eng.auburn.edu/~pjones/MECH.5830.6830.6836/Internal_Combustion_Engines_Fundamentals_by_J.B.Heywood.pdf)
- Anonymous 9: <https://en.demotor.net/heat-engine/differences-otto-and-diesel-engine>
- Anonymous 10: <https://www.sciencedirect.com/topics/engineering/compression-ignition-engine>
- Anonymous 11: <http://www.mechanicalbooster.com/2014/02/how-does-a-four-stroke-diesel-engine-or-compression-ignition-engine-work.html>
- Anonymous 12: [https://www.researchgate.net/figure/The-diesel-engine-cycle\\_fig4\\_260878177](https://www.researchgate.net/figure/The-diesel-engine-cycle_fig4_260878177)
- Anonymous 13: <http://www.ijmerr.com/uploadfile/2015/0409/20150409042911754.pdf>
- Anonymous 14: <https://www.nettinc.com/information/emissions-faq/what-are-diesel-emissions>
- Anonymous 15: <https://www.eea.europa.eu/data-and-maps/indicators/eea-32-sulphur-dioxide-so2-emissions-1/assessment-3>
- Anonymous 16: [http://naei.beis.gov.uk/overview/pollutants?pollutant\\_id=8](http://naei.beis.gov.uk/overview/pollutants?pollutant_id=8)
- Anonymous 17: <https://www.environment.gov.au/protection/publications/factsheet-sulfur-dioxide-so2>

- Anonymous 18: [https://www.ripublication.com/ijaer18/ijaerv13n6\\_08.pdf](https://www.ripublication.com/ijaer18/ijaerv13n6_08.pdf)
- Anonymous 19: <https://x-engineer.org/automotive-engineering/internal-combustion-engines/performance/air-fuel-ratio-lambda-engine-performance/>
- Anonymous 20: <https://mde.maryland.gov/programs/Air/MobileSources/Pages/DieselHealthandEnvironmentalEffects.aspx>
- Anonymous 21: <https://www.eea.europa.eu/publications/explaining-road-transport-emissions>
- Anonymous 22: <https://mde.maryland.gov/programs/Air/MobileSources/Pages/DieselHealthandEnvironmentalEffects.aspx>
- Anonymous 23: <http://www.icopal-noxite.co.uk/nox-problem/nox-pollution.aspx>
- Anonymous 24: [http://www.theicct.org/sites/default/files/publications/ICCT\\_G20-briefing-paper\\_Jan2017\\_vF.pdf](http://www.theicct.org/sites/default/files/publications/ICCT_G20-briefing-paper_Jan2017_vF.pdf)
- Anonymous 25: [https://www.continental-automotive.com/getattachment/8f2dedad-b510-4672-a005-3156f77d1f85/Emission\\_Booklet\\_2017.pdf](https://www.continental-automotive.com/getattachment/8f2dedad-b510-4672-a005-3156f77d1f85/Emission_Booklet_2017.pdf)
- Anonymous 26: <https://www.transportpolicy.net/standard/eu-heavy-duty-emissions/>
- Anonymous 27: [https://ec.europa.eu/growth/sectors/automotive/environment-protection/emissions\\_en](https://ec.europa.eu/growth/sectors/automotive/environment-protection/emissions_en)
- Anonymous 28: <https://www.sciencedirect.com/topics/engineering/emission-regulation>
- Anonymous 29: <http://ec.europa.eu/environment/air/transport/road.htm>
- Anonymous 30: [https://commons.wmu.se/cgi/viewcontent.cgi?article=1297&context=all\\_dissertations](https://commons.wmu.se/cgi/viewcontent.cgi?article=1297&context=all_dissertations)
- Anonymous 31: [https://www.dieselnet.com/tech/engine\\_egr.php](https://www.dieselnet.com/tech/engine_egr.php)
- Anonymous 32: <http://www.hillsidemechanicaland4x4.com/dpfinfo>

- Anonymous 33: [http://www.kelberg.com/downloads/daf\\_e6.pdf](http://www.kelberg.com/downloads/daf_e6.pdf)
- Anonymous 34: <https://www.honestjohn.co.uk/faq/diesel-particulate-filters/>
- Anonymous 35: <https://www.sciencedirect.com/topics/engineering/catalytic-converters>
- Anonymous 36: <https://www.research-collection.ethz.ch/bitstream/handle/20.500.11850/49450/eth-27993-02.pdf>
- Anonymous 37: <https://www.nettinc.com/information/emissions-faq/how-does-a-three-way-catalyst-work>
- Anonymous 38: <https://books.google.com.tr/books?id=Kd0kBAAAQBAJ&pg=PA38&lpg=PA38&dq=At+high+exhaust+temperatures,+DOC+can+provide+effective+control+of+HC+and+CO+emissions+with+reduction+efficiencies+in+excess+of+90%25.&source=bl&ots=wasL8RcpME&sig=ACfU3U1TLdRHJVWfW2xZehR6IQaJDQdKw&hl=tr&sa=X&ved=2ahUKEwi4kNC52N7iAhUI8hoKHY8cA2EQ6AEwAXoECAkQAQ#v=onepage&q=At%20high%20exhaust%20temperatures%2C%20DOC%20can%20provide%20effective%20control%20of%20HC%20and%20CO%20emissions%20with%20reduction%20efficiencies%20in%20excess%20of%2090%25.&f=false>
- Anonymous 39: <http://www.attacproject.eu/facts-on-diesel-oxidation-catalysts/>
- Anonymous 40: <http://www.solvents.basf.com/portal/streamer?fid=278929>
- Anonymous 41: <https://www.sigmaaldrich.com/chemistry/solvents/2propanol-center.html>
- Anonymous 42: <https://www.greenchem-adblue.com/informations/what-is-adblue/>
- Anonymous 43: <https://www.lenntech.com/periodic/elements/pd.htm>

## **CURRICULUM VITAE**

Osman Cenk Candemir was born in Seyhan, Adana in September 1988. He graduated from Seyhan ÇEAŞ Anatolian High School in 2007. After this, he started his BSc degree in the following year at Çukurova University, Mechanical Engineering Department and graduated in 2013. He started his MSc education in the Automotive Engineering department of the same University in 2015. He had studied for his thesis project at Çukurova University, Automotive Engineering Department.